THE SOLAR ORIGIN OF COROTATING INTERACTION REGIONS AND THEIR FORMATION IN THE INNER HELIOSPHERE

Report of Working Group 1

A. BALOGH[1] AND V. BOTHMER[2]
CO-CHAIRS

N. U. CROOKER[3], R. J. FORSYTH[1], G. GLOECKLER[4,5], A. HEWISH[6], M. HILCHENBACH[7], R. KALLENBACH[8], B. KLECKER[9], J. A. LINKER[10], E. LUCEK[1], G. MANN[11], E. MARSCH[7], A. POSNER[2], I. G. RICHARDSON[4,12], J. M. SCHMIDT[1], M. SCHOLER[9], Y.-M. WANG[13], AND R. F. WIMMER-SCHWEINGRUBER[14]
PARTICIPANTS

M. R. AELLIG[14], P. BOCHSLER[14], S. HEFTI[5], AND Z. MIKIĆ[10]
CONTRIBUTING AUTHORS NOT PARTICIPATING IN THE WORKSHOP

[1]*The Blackett Laboratory, Imperial College, London, United Kingdom*
[2]*Extraterrestrische Physik, Universität Kiel, Kiel, Germany*
[3]*Center for Space Physics, Boston University, Boston, Massachussetts, USA*
[4]*Dept. of Physics and IPST, University of Maryland, College Park, Maryland, USA*
[5]*Dept. of Atmosph., Oceanic, and Space Sciences, University of Michigan, Ann Arbor, Mich., USA*
[6]*Mullard Radio Astronomy Observatory, Cavendish Laboratory, Cambridge, United Kingdom*
[7]*Max-Planck-Institut für Aeronomie, Katlenburg-Lindau, Germany*
[8]*International Space Science Institute, Bern, Switzerland*
[9]*Max-Planck-Institut für Extraterrestrische Physik, Garching, Germany*
[10]*Science Applications International Corporation, San Diego, California, USA*
[11]*Astrophysikalisches Institut, Potsdam, Germany*
[12]*NASA/Goddard Space Flight Center, Greenbelt, Maryland, USA*
[13]*E.O. Hulburt Center for Space Research, Naval Research Laboratory, Washington, DC, USA*
[14]*Physikalisches Institut der Universität Bern, Bern, Switzerland*

Received: March 31 1999; Accepted: June 30 1999

Abstract. Corotating Interaction Regions (CIRs) form as a consequence of the compression of the solar wind at the interface between fast speed streams and slow streams. Dynamic interaction of solar wind streams is a general feature of the heliospheric medium; when the sources of the solar wind streams are relatively stable, the interaction regions form a pattern which corotates with the Sun. The regions of origin of the high speed solar wind streams have been clearly identified as the coronal holes with their open magnetic field structures. The origin of the slow speed solar wind is less clear; slow streams may well originate from a range of coronal configurations adjacent to, or above magnetically closed structures. This article addresses the coronal origin of the stable pattern of solar wind streams which leads to the formation of CIRs. In particular, coronal models based on photospheric measurements are reviewed; we also examine the observations of kinematic and compositional solar wind features at 1 AU, their appearance in the stream interfaces (SIs) of CIRs, and their relationship to the structure of the solar surface and the inner corona; finally we summarise the Helios observations in the inner heliosphere of CIRs and their precursors to give a link between the optical observations on their solar origin and the in-situ plasma observations at 1 AU after their formation. The most important question that remains to be answered concerning the solar origin of CIRs is related to the origin and morphology of the slow solar wind.

Space Science Reviews **89:** 141–178, 1999.

1. Introduction

A. BALOGH, V. BOTHMER, R. KALLENBACH

The solar wind that pervades the heliosphere is the interplanetary extension of the Sun's outer atmosphere, the solar corona. It is now widely accepted that there are two distinct kinds of solar wind emitted from the Sun, distinguished by their different speeds, densities, elemental and isotopic composition, as well as their kinetic and coronal freeze-in temperatures. Fast (typically $>$ 600 km/s) solar wind is known to be emitted from large coronal holes which have an open magnetic field structure, although the acceleration mechanism remains uncertain. The coronal origin of the slow solar wind (typically $<$ 400 km/s) remains debated even though it is well established that it is related to regions near magnetically closed coronal structures and the streamer belt (see Fig. 1). As it will be pointed out in more detail in this article the differentiation between solar wind types based on speed alone is an oversimplification. Solar wind streams which originate in coronal holes are imprinted with the lower coronal temperatures and other compositional signatures of the regions in which they originate. However, at least near the ecliptic, such streams can have, occasionally, significantly lower speeds, less than 500 km/s. While the two kinds of solar wind can be observationally distinguished, within each kind (but more so in the case of the slow solar wind) there is an inherent variability of all the bulk flow parameters, as well as in composition (see Sect. 3 of this chapter, also Forsyth and Marsch, 1999, this volume). The distribution of the two kinds of solar wind types in the corona varies considerably on many time scales, of which the solar cycle is the dominant one.

The structure of the heliosphere is determined in part by the spatial and temporal dependence of coronal structures from which slow and fast solar wind streams are emitted and in part by the dynamics of interacting non-uniform solar wind flows in the heliosphere. Corotating Interaction Regions (CIRs) constitute an important set of large scale structures in the heliosphere observed in the declining and minimum phases of the solar activity cycle (see, *e.g.* Gosling and Pizzo, 1999, this volume, and references therein). A discussion of the solar origin of CIRs involves the identification of the distribution of the two kinds of solar wind in the corona which leads to their formation.

Given the very large scale and quasi-stationary nature of CIRs, we are looking for correspondingly large scale and equally quasi-stationary patterns in the corona. The zeroth order approximation for the solar wind is the original model of Parker (1958) in which the solar wind has a uniform, time-independent velocity over the whole Sun. As a first order approximation, a model can be constructed in which fast solar wind at constant speed is emitted from time-stationary coronal holes surrounding the poles of the sun, and slow solar wind, also at constant speed, is emitted from a band (limited in latitude to about 20 to 30 degrees south and north) around the solar magnetic equator. This first order model is known, from Ulysses observations made in 1993 to 1996, to be reasonably accurate in the late declining

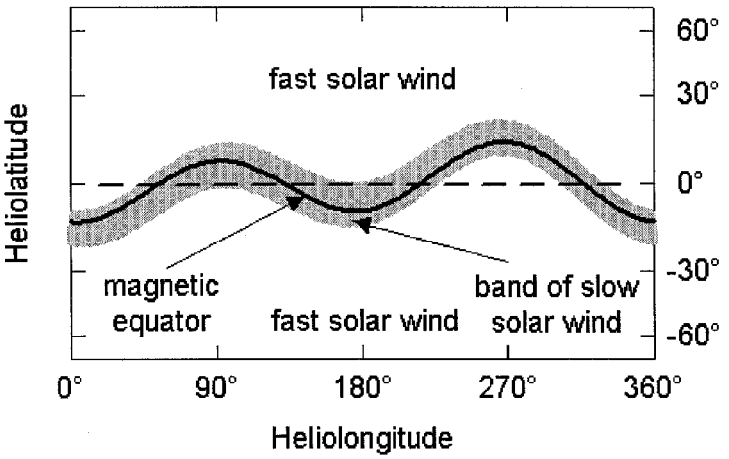

Figure 1. A schematic representation of the solar wind source function in the declining and minimum phases of the solar activity cycle. The distribution of the two kinds of solar winds is shown at a nominal distance from the Sun where dynamic effects in the corona no longer affect the solar wind speed. The complexity of the transition region between fast and slow solar wind regions is not illustrated here.

and minimum phases of the solar activity cycle. From what we know from near-ecliptic missions, during the rising and maximum phases of the solar activity cycle, the solar wind at nearly all latitudes appears to be of the slow kind (with highly variable bulk parameters) with a significant addition of transient material from Coronal Mass Ejections (CMEs). The survey in heliolatitude to confirm that this is the case everywhere around the Sun remains to be done; Ulysses will perform the necessary observations during the forthcoming activity maximum.

The first order model of the solar wind sources, valid in the declining and minimum phases of the solar cycle, allows the large scale modelling of the interaction between fast and slow solar wind streams (*cf.* Gosling and Pizzo, 1999, this volume, and references therein) which occurs in interplanetary space. In this model, the band of slow solar wind surrounds the solar magnetic equator, rather than the heliographic equator. The magnetic equator is tilted with respect to the heliographic equator and a consequence of this model is that, at a given heliolatitude, up to about 30 degrees north and south of the solar (heliographic) equator, fast and slow solar wind streams can alternate as a function of heliolongitude, with one or at most two stream pairs around the Sun. The interpretation of observations of Corotating Interaction Regions (CIRs) is effectively based on this first order model of solar wind sources. This argument can also be reversed: the observation of CIRs in and near the solar equator in interplanetary space implies the near-stationarity of the solar wind sources, in the form of alternating fast and slow streams which recur at a given longitude with the solar rotation period. This solar wind source pattern is a necessary and sufficient condition for the development of large scale interaction regions which form a stationary, corotating pattern in interplanetary space.

The main reservation concerning the validity of this simple model is that temporal evolution in coronal structures, in particular along the boundaries of coronal holes, still occurs during these phases of the solar cycle. Although very long-lived coronal holes have been observed, resulting in the relatively steady fast solar wind streams, strict stationarity of the solar wind sources can only be an approximation. An additional reservation is that while the transition region between fast and slow solar wind sources may be abrupt, it is clearly not a step function and its structure may well be complex and variable, thus likely to result in a range of dynamic effects in the corona which shape the interaction of the streams in interplanetary space.

Coronal structure, the context for the origin of the different solar wind streams, is in turn determined by the solar magnetic field. It is the variation of the global magnetic field of the Sun that leads to the approximately 11-year solar cycle variation in the magnetic structure of the corona. In the declining phase of the solar cycle, the dipole term of the global magnetic field increases in relative importance, with a simultaneous, meridional rotation of the dipole axis towards the solar rotation axis. This dipole term, together with some remaining quadrupolar contribution, dominates the large scale structure of the Sun's magnetic field up to and just beyond solar minimum. This simple picture of the coronal magnetic fields, leading to the distribution of solar wind sources in the corona at the origin of CIRs, is discussed in greater detail in Sect. 2 of this chapter. In that section, it is shown how models of the solar corona using observed photospheric magnetic fields as the boundary conditions can reproduce many aspects of coronal structure, and how these models can also be used to infer the solar origin of features observed in the solar wind. The way in which time-dependent changes to coronal magnetic fields may allow material in previously closed regions to escape into the solar wind is also discussed in Sect. 2.

If, on a simplified level, CIRs arise because of the relatively abrupt transition between coronal regions in which the fast and slow solar wind originate, dynamic modelling would be able, in principle, to reproduce not only the main structural characteristics of CIRs (Gosling and Pizzo, 1999, this volume), but also the details of the interaction at the interface between the compressed slow solar wind followed by the fast solar wind stream. While interfaces within many CIRs have been recognised, not all streams contain identifiable interfaces. The existence, in general, of SIs and their development over heliocentric distance from a fraction of an AU to 5 AU and beyond remains to be clarified. As will be pointed out in Sect. 3, CIRs are a consequence of flow speed differences between the two types of solar wind. It is possible to envisage the formation of interaction regions by sufficiently steep velocity gradients in solar wind speed from within the same coronal hole regions, when an interface would not be expected to form, at least not in compositional terms. However, Wimmer-Schweingruber *et al.* (1997) demonstrated congruity between the traditional density and temperature (Gosling *et al.*, 1978) and the compositional signatures, and Burton *et al.* (1999) used continuous Ulysses data

from June 1992 to July 1993 to confirm this congruity including the trailing edge solar wind SIs.

In this paper, we mainly pay attention to the coronal signatures of SIs: for detailed discussions of SIs, see Gosling *et al.* (1978), Wimmer-Schweingruber *et al.* (1997), also Gosling and Pizzo (1999), Crooker, Gosling *et al.* (1999) and references therein. In Sect. 3, the identification of interfaces and boundaries in general is discussed further, mostly in terms of compositional changes in the parameters of the solar wind and their relation to solar and coronal features. Compositional observations provide important complementary evidence on the nature of the slow-fast interface in CIRs, and also on the nature of the boundary between slow and fast solar wind streams in the corona. In addition, compositional changes provide a tool to examine in more detail the structure within fast and slow solar wind.

It is recognised here that the current debate concerning the nature and origin of the slow solar wind is relevant to the understanding of both the larger scale characteristics of CIRs and the interface between the fast and slow wind streams where the interaction takes place.

One approach to explain the high variability of slow solar wind streams is in terms of their generally more complex filamentary structure compared to fast solar wind streams (*e.g.* Gosling, 1997). As discussed in Sect. 3, there is observational evidence from composition data that a filament corresponding to the size of a supergranular cell can be identified even out at a heliocentric distance of 1 AU.

On the larger scale, the model of field line transport by Fisk *et al.* (1998) (see also Fisk and Jokipii, 1999, in this volume) based on the differential rotation of the photosphere, the tilt of the Sun's magnetic dipole axis and the super-radial expansion of the solar wind may imply the reconnection of field lines at the edges of coronal holes, continuously opening up previously closed coronal loops. This model for the origin of the slow solar wind would explain the great variability of its characteristic parameters as different loop systems presumably release plasmas of different characteristics. The possibility that this mechanism also leads to a fragmentary structure within the slow solar wind near its boundary with the fast streams from the nearby coronal holes introduces a considerable degree of potential complexity near the slow-fast interface in CIRs. For the time of solar minimum, however, it is evident from composition measurements that most of the slow solar wind originates from the roots of the coronal loops flowing along open field lines at their periphery (von Steiger, 1998). The best-known example for a type of fragmentary structure during solar minimum is the CME-related solar wind which sometimes shows very unusual composition (Gloeckler *et al.*, 1999). Compositional boundaries between the CME-related and the quasi-stationary slow solar wind are not or need not be SIs such as observed in CIRs or related to fast-slow interactions in general, but they show many similar signatures. The presumably cycle-dependent relevance of the transient types of solar wind for the large-scale structure of the solar wind and the CIRs remains to be examined in detail during the forthcoming solar maximum possibly by multi-spacecraft observations.

On the other hand, the importance of this view in the context of CIRs is that evidence for the model is best sought at the slow-fast interfaces within CIRs, and that compositional data, supplemented by other evidence for the fragmentary nature of the slow solar wind stream are important for understanding the solar origin of CIRs. An important requirement on this, as well as on alternative models of the origin of the slow solar wind is the need to provide an explanation of the large degree of variability in kinematic and compositional parameters.

Given the variety of CIRs observed both at 1 AU and beyond, it is clear that their early evolution from the corona to 1 AU is of decisive importance in shaping the structures which reach their full development, in general, at 2 to 4 AU. The observations by the two Helios spacecraft between 0.3 and 1 AU in the 1970s remain a unique data set in the inner heliosphere. In Sect. 4, we summarize the principal results of the Helios observations related to stream-stream interactions, their relationship to coronal structure, and their relationship to energetic particles and cosmic rays.

A summary of the questions and conclusions by this Working Group are presented in the final section of this chapter.

2. The Relationship of Fast and Slow Solar Wind to Coronal Structure

J. A. LINKER, Y.-M. WANG, E. MARSCH, A. POSNER, V. BOTHMER, Z. MIKIĆ

As mentioned in the introduction, the solar wind that pervades the heliosphere is the interplanetary extension of the Sun's outer atmosphere, the solar corona. Thus it is not surprising that coronal structure strongly influences heliospheric structure. Coronal structure is in turn primarily controlled by the Sun's magnetic field. The complexity of the Sun's global magnetic field varies with the approximate 11-year solar cycle, and this level of complexity is reflected in the structure of the solar corona. During solar minimum, the corona typically exhibits a well-defined streamer belt with coronal holes in the polar regions, and these structures may persist over several rotations. It is this reasonably well-ordered structure of the solar minimum corona that gives rise to CIRs in the heliosphere.

Coronal holes are known to be regions of open magnetic field where the solar wind expands outward. The solar wind is far from uniform, and is often described as being either 'slow' (300–500 km/s) or 'fast' (600–800 km/s) although speed alone is not a sufficient parameter to characterise the two types of streams as outlined in the introduction and discussed further in Sect. 3. The mechanism(s) that are ultimately responsible for accelerating fast solar wind streams and creating the dichotomy of fast and slow wind are poorly understood. However, measurements from the Ulysses spacecraft have demonstrated that uniformly fast solar wind is present at the poles of the Sun during the declining phase of the solar activity cycle and at solar minimum (Phillips *et al.*, 1995), while a mixture of slow and fast solar wind is observed to dominate near the ecliptic plane. Polar coronal holes are

typically not azimuthally symmetric structures, but instead their center is displaced from the Sun's rotation axis. This sometimes allows fast solar wind streams which in addition have warps and dips to be present near lower heliographic latitudes where the slow solar wind predominates. This intermingling of fast and slow solar wind streams is the genesis of the CIRs observed farther out in the heliosphere because outward from the Sun to 1 AU fast wind streams begin to catch up with slow wind streams.

In this section, we focus on the role of the Sun's magnetic field in defining the structure of the solar minimum corona and inner heliosphere. We show how models of the solar corona using observed photospheric magnetic fields as boundary conditions can reproduce many aspects of coronal structure, and how these models can also be used to infer the solar origin of features observed in the solar wind. We also discuss how time-dependent changes to coronal fields may allow material in previously closed regions to escape into the solar wind.

2.1. Coronal Structure Near Solar Minimum

A fundamental difficulty in understanding coronal structure is that, while the magnetic field is believed to play a central role, there are few measurements of the coronal magnetic field. However, the line-of-sight component of the magnetic field has been measured in the photosphere for many years (for example, at the Wilcox Solar Observatory and at the National Solar Observatory at Kitt Peak). If we are to understand the role of the magnetic field in producing coronal structure, we must use the measured photospheric field to infer the coronal field. The simplest and most widely used techniques for accomplishing this task are based on potential field models (*e.g.*, the potential field source-surface model, Schatten *et al.*, 1969; Altschuler and Newkirk, 1969; and the potential field current-sheet model, Schatten, 1971). These models have been used extensively in the analysis of coronal and interplanetary data (*e.g.*, Hoeksema *et al.*, 1983; Wang and Sheeley, 1988; 1992; 1995). Recently, magnetohydrodynamic (MHD) calculations have advanced to the point where they can also incorporate observed photospheric magnetic fields into the boundary conditions to produce realistic models of the solar corona (Mikić and Linker, 1996; Usmanov, 1996; Linker *et al.*, 1996; 1999). In this approach, the time-dependent MHD equations are integrated in time until a steady-state is reached. The final equilibrium solution gives a representation of the coronal plasma and magnetic fields for the time period of interest.

One advantage of the MHD approach is that because the equations also describe the coronal plasma, the results can be tested against white light observations. A typical example is shown in Fig. 2. Here an MHD computation was carried out using photospheric magnetic field data from Kitt Peak for Carrington Rotation 1892 (January 27–February 23, 1995). Figure 2(a) shows the polarization brightness (pB) observed with the High Altitude Observatory's MKIII Coronameter at Mauna Loa for 3 days during February, 1995. By integrating the plasma density

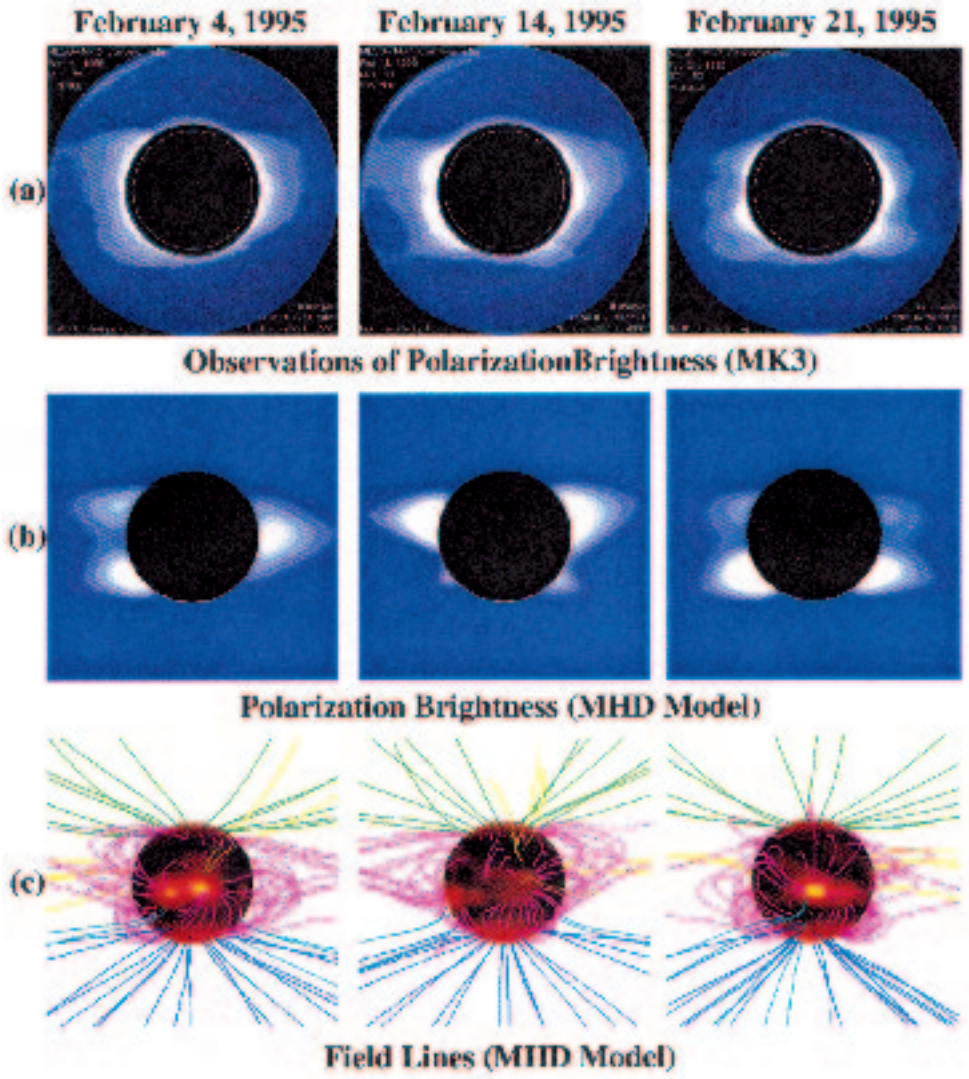

Figure 2. Comparison of the MHD model of the solar corona for CR1892 (Linker and Mikiċ, 1997) with daily white-light coronal images. (a) Images of the polarisation brightness *pB* from the Mauna Loa Solar Observatoty (MLSO) Mark III K-coronameter, for 4 days during the Whole Sun Month time period. (b) The *pB* predicted by the MHD computation for the same days shown in (a). (c) Magnetic field lines from the MHD computation for the same days shown in (a) and (b). Purple field lines are closed, the others are open.

from the MHD calculation convolved with a scattering function (Billings, 1966), we can compute the pB predicted by the MHD calculation, as shown in Fig. 2(b). Note that the predicted pB agrees quite well with the observations. Figure 2(c) shows the magnetic field lines from the calculation. As expected, the streamer belt corresponds to a region of closed field lines.

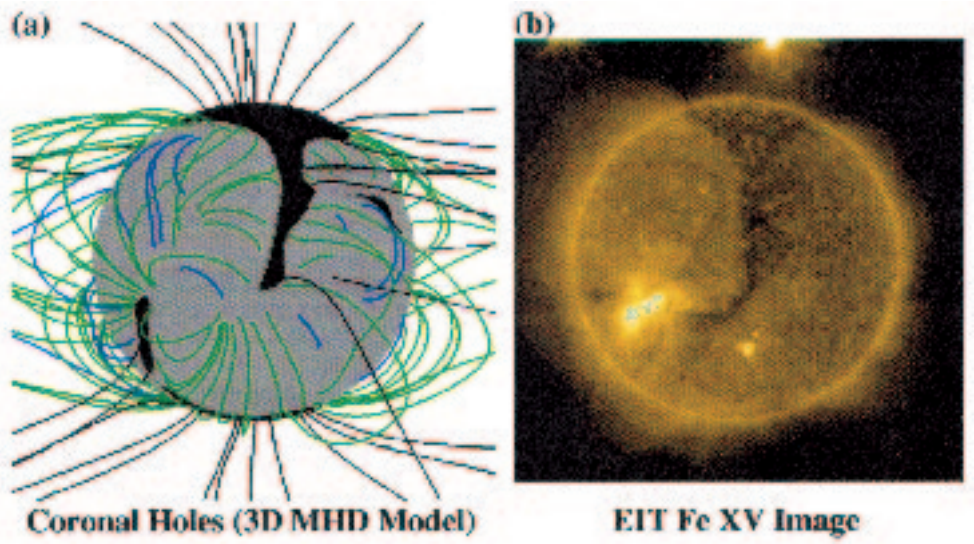

Figure 3. (a) Coronal holes (open field regions, shown in black) from an MHD model of the solar corona for Whole Sun Month, as would be visible on August 27, 1996. Closed field regions are gray. (b) An EIT FeXV image for the same day. The "elephant's trunk" coronal hole is clearly visible in the EIT image and has been reasonably captured by the model.

Another way that coronal models can be tested is by comparing them with disk images. When the disk of the Sun is viewed in emission lines such as extreme ultraviolet or soft X-rays, coronal holes appear dark as compared with other regions of the solar atmosphere, because the plasma in coronal holes is cooler and less dense than the streamer belt plasma. Figure 3 shows a comparison of open-field regions from the MHD calculation (shown in black; closed-field regions are gray) with SOHO EIT (Extreme Ultraviolet Imaging Telescope) images on August 27, 1996. A coronal hole extending from the solar north pole to the equator was visible at this time in EIT (and other observations as well); this coronal hole has been referred to as the 'elephant's trunk'. Note that the observed coronal hole corresponds with a region of open magnetic field in the MHD model. Source-surface models (Zhao *et al.*, 1999) are also capable of reproducing the coronal holes reasonably well, suggesting that coronal hole boundaries are primarily determined by the photospheric magnetic field. These observations occurred during Whole Sun Month (WSM; August 10 – September 8, 1996) during which time a wide range of solar observations were obtained; Linker *et al.* (1999) describe more detailed comparisons for this time period.

The results shown thus far indicate that models of the coronal magnetic field based on observed photospheric magnetic fields can capture many of the basic features of the solar-minimum corona. These results support the long held belief that the shape of the streamer belt and coronal hole are strongly influenced by the photospheric magnetic field. As the solar wind carries the imprint of this structure

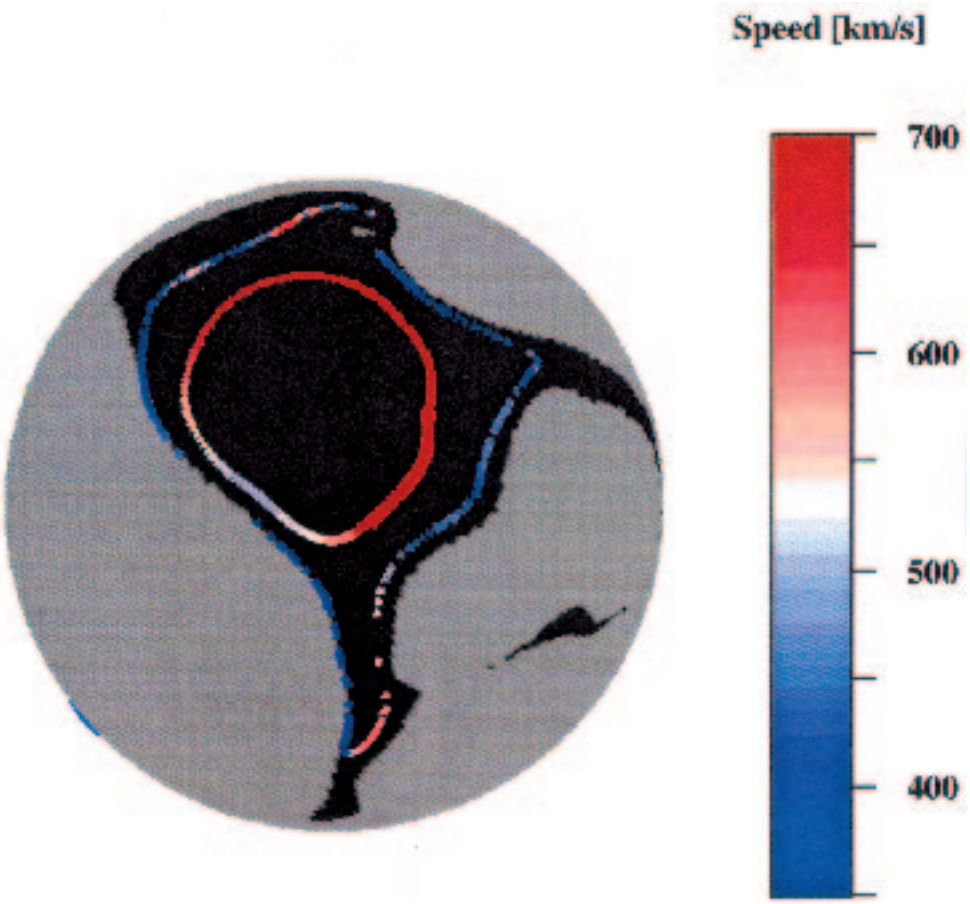

Figure 4. Mapping of solar wind velocity measurements during Whole Sun Month from Ulysses (inner trace at high latitude) and WIND (lower latitude trace) back to the Sun. Solar wind speed is color coded with the largest red and smallest blue. The coronal hole boundaries from the MHD model are shown in the same format as Fig. 3, but viewed from above the north pole of the Sun.

out into the heliosphere, we can use models to infer information about the source location of solar wind features, as described in the next section.

2.2. Mapping of Solar Wind Measurements Back to the Sun

If a coronal magnetic field model approximates the true field reasonably well, it can be used to investigate the source locations of solar wind features. For the WSM time period discussed above, Linker *et al.* (1999) used a ballistic approximation to map solar wind features into the domain of the MHD calculation, then used the MHD results to map the source back to the Sun. Figure 4 shows the mapping of solar wind velocity measurements from the WIND and Ulysses spacecraft. A general trend one sees in Fig. 4 is that slow wind velocity usually maps back to regions near coronal hole boundaries, while fast wind typically comes from deeper

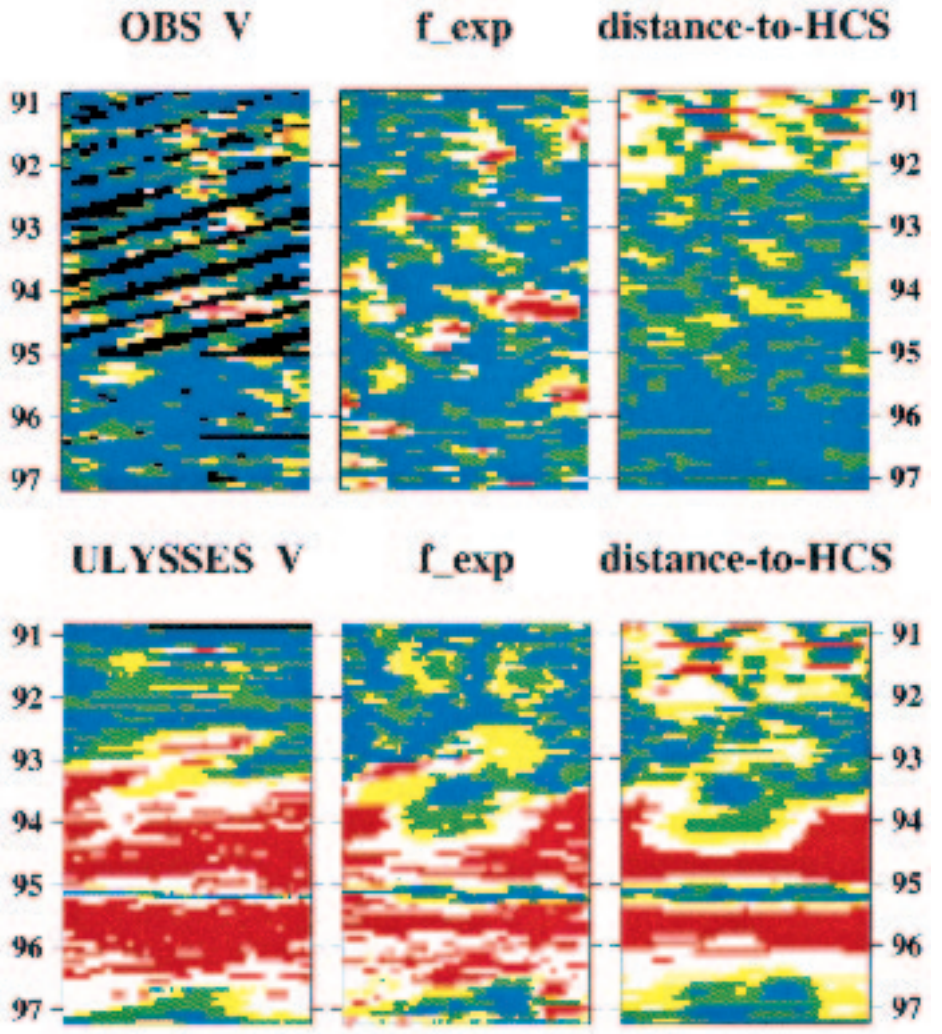

Figure 5. Stackplots of the solar wind speed measured at 1 AU and at Ulysses (left panels, top and bottom, respectively) as a function of heliolongitude from 1991 to 1997; the centre panels show the solar wind speeds predicted, using the calculated coronal expansion factor; the right panels show the solar wind speeds calculated, based on the distance of the observers from the coronal imprint of the Heliospheric Current Sheet, at 1 AU and Ulysses, respectively. Note the generally better match between observations and the coronal expansion factor model (based on Wang *et al.*, 1997).

within coronal holes. The empirical relationship between solar wind velocity and the expansion of coronal magnetic flux tubes has been investigated extensively by Wang and Sheeley (1990; 1994; 1995) and Wang *et al.* (1997). An inverse correlation has been found between the coronal expansion factor and the speed of the solar wind measured at 1 AU; this anti-correlation was further confirmed by solar wind measurements along the polar orbit of Ulysses (see Fig. 5). In this empirical model,

the coronal expansion factor is defined as the ratio of the areas of magnetic flux tubes at the radial distance of the source surface of PFSS (potential field, source surface model of the corona as defined above, with the radius of the source surface taken to be 2.5 $R_\odot$) and the photosphere. In quantitative terms, this expansion factor is largest ($>$20) near the boundaries of coronal holes, where the open flux tubes expand greatly, draped over the closed field structures of the streamer belt (as is also apparent in Fig. 2). By contrast, the expansion factor is smallest ($<$4.5) in the central regions of the coronal holes. The distribution of intermediate values of the expansion factor depends on the relative topology of coronal holes. The highest solar wind velocities correspond to the smallest expansion factors, while the slow solar wind appears to be associated with regions where the expansion factor is the largest.

The anticorrelation between solar wind speed and the expansion factor calculated from the PFSS model of the coronal distribution of magnetic flux can be used to predict solar wind speeds. A comparison of the predicted and observed solar wind speeds at 1 AU (Wang and Sheeley, 1994), and along the solar polar orbit of Ulysses (Wang *et al.*, 1997) has shown that there is a general qualitative agreement between solar wind speeds calculated from the expansion factors and the patterns of high and low solar wind speeds measured at both 1 AU and at Ulysses. However, the solar wind speeds predicted from the expansion factors show larger speed gradients than observed; in particular, the predicted high speed streams have a higher velocity than the measured wind speeds in the ecliptic. This is illustrated in Fig. 5, where, in addition to the observed wind speeds (left panels), the wind speeds calculated using the coronal expansion factor (centre panels) are shown from 1990 to 1997. This discrepancy is likely to be at least in part due to the interaction of the slow and fast wind streams: fast streams are slowed down by their interaction with preceding slow streams within the equatorial regions, so that the observed speed gradients are reduced at latitudes where both slow and fast streams are present. In the right panels, predicted solar wind speeds are shown, assuming an alternative model based on the dependence on the angular distance of the points of observation to the Heliospheric Current Sheet (HCS). This latter model clearly does not match the observations, in particular around solar maximum.

Mapping techniques have also been used to study the magnetic connection of recurrent energetic particle events. COSTEP energetic proton flux enhancements, compressions and solar wind speed increases track each other over several Carrington rotations and can be correlated with synoptic maps in 195 Å by EIT. Figure 6, taken from Posner *et al.* (1999), shows the mapping of SOHO/COSTEP observations during WSM. The CIR-associated particle events are correlated with the extensions of the northern polar coronal hole boundaries.

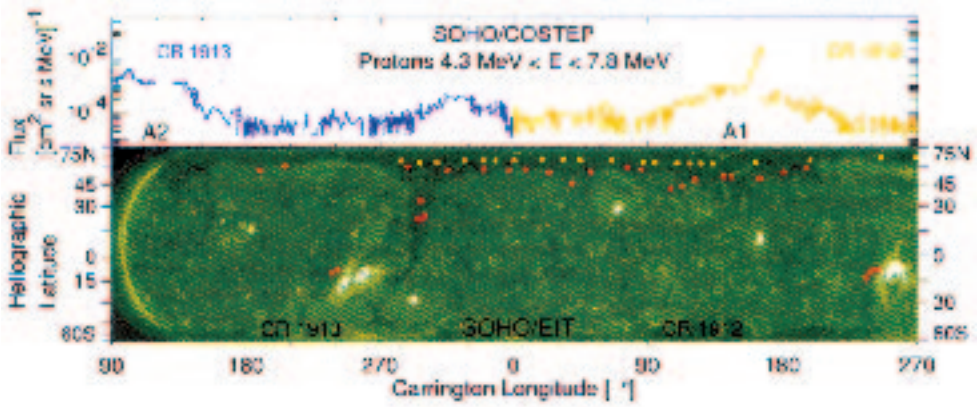

Figure 6. Mapping of SOHO/COSTEP proton measurements during Whole Sun Month back to the Sun. The position of SOHO on the green synoptic map by EIT is shown in red, Ulysses in yellow.

2.3. Time-Dependent Nature of the Corona and Solar Wind

While steady-state coronal models help give insight into overall coronal structure, in reality the corona is changing continuously, even during times of solar minimum. This changing structure is driven by changes in the photospheric magnetic field; active regions emerge and disperse continuously during the solar cycle. The MHD model can incorporate the evolution of the photospheric magnetic field, so that the corresponding evolution of the corona can be followed.

To study the evolution of the corona during the period Feb. 1, 1997–Mar. 18, 1998 (15 Carrington rotations), Mikić *et al.* (1999) used a sequence of synoptic Kitt Peak observations to specify magnetic flux evolution at the photosphere during the time interval. In order to study the quasi-static evolution of the corona for more than a year's worth of data, the photospheric magnetic field was changed at a rate that was enhanced by approximately ten times compared to real time. This approximation makes it impossible to study the detailed evolution of individual events, though it is still meaningful to study the quasi-static evolution of the large-scale structure of the corona. For the a.m. time period Fig. 7 shows the evolution of the streamer structure, the HCS, and the coronal hole boundaries which are the origin of kinematic and compositional signatures of SIs in CIRs described in Sect. 3 below. Note the increase in complexity of the coronal magnetic field as the Sun emerges from solar minimum.

A conspicuous feature of the simulated coronal evolution is the sporadic opening of previously closed field regions as the magnetic flux on the Sun is rearranged. These results imply that at times the streamer belt plasma (which cannot escape the inner corona in the steady-state picture) is carried out into the solar wind. Periodic reconnection at coronal hole boundaries could form the "blobs" discussed by Wang *et al.* (1997; 1998) or even the CMEs; for CMEs this dispersal of streamer belt plasma into the slow solar wind is known to be the source of compositional signatures also discussed in the next section.

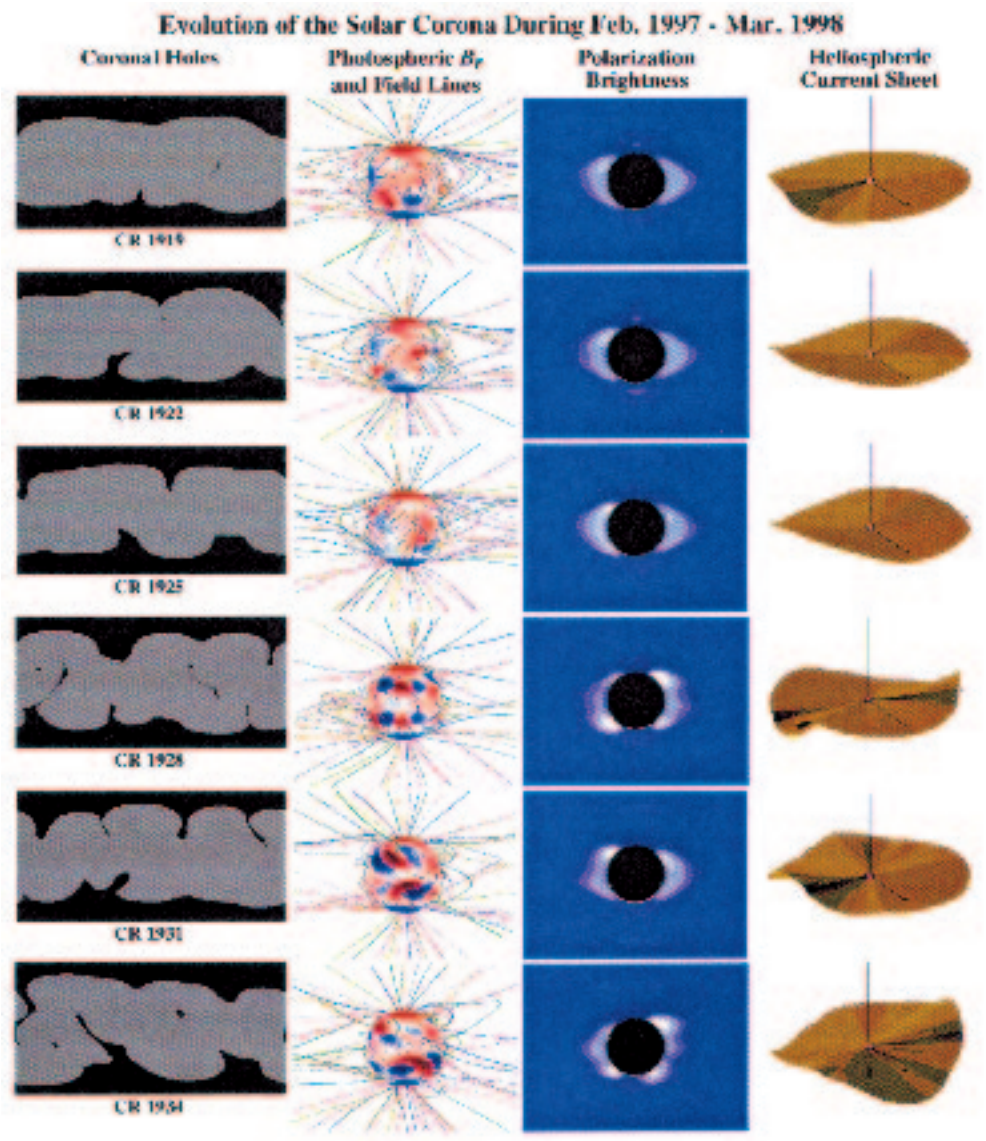

Figure 7. The changing structure of the solar corona during the period Feb. 1997–Mar. 1998 (Carrington rotations 1919-1934), as illustrated by coronal hole maps (longitude vs. latitude, with gray/black indicating closed/open field regions), field line traces with the radial magnetic field shown on the surface of the Sun (blue areas denote field lines directed into, red areas field lines out of the Sun, respectively), polarization brightness, and the shape of the heliospheric current sheet. This time period represents the rising phase of the new solar cycle. The photospheric magnetic field was set as a time-dependent boundary condition on the 3D MHD simulation using Kitt Peak synoptic maps (Mikiċ *et al.*, 1999).

3. Compositional and Kinematic Signatures of Solar Wind Stream Interfaces and Their Relationship with Solar and Coronal Features

R. KALLENBACH, M. AELLIG, P. BOCHSLER, N. U. CROOKER, R. J. FORSYTH, S. HEFTI, M. HILCHENBACH, R. F. WIMMER-SCHWEINGRUBER

The formation of a CIR is caused by the speed differences of fast and slow solar wind and the solar rotation. In this section we characterise the different kinematic and compositional signatures of the two types of coronal outflow and their relationship to solar features as well as their appearance in the SIs of CIRs. Within many CIRs SIs have been recognised in terms of the criteria discussed in more detail by Wimmer-Schweingruber *et al.* (1997) and Crooker, Gosling *et al.* (1999) in this volume. These criteria include abrupt changes in speed, density, temperature (entropy), and composition. The evolution of these quantities has been analyzed at 1 AU in the ecliptic mix of slow and fast solar wind with a time resolution of 5 minutes using data of the CELIAS experiment (Hovestadt *et al.*, 1995) on board the SOHO spacecraft. From this analysis conclusions are drawn on the persistence of the solar wind over a solar rotation. Also, the persistence of kinematic and compositional signatures on their way from a few solar radii out to 1 AU has been studied, and an upper limit for the cross-field diffusion in the solar wind is given. Whereas the persistence of speed differences is essential for the formation and persistence of the CIRs, the high persistence of the compositional signatures complements the set of precise diagnostic tools for the SIs in CIRs. In addition to the variable He/H abundance ratio in the solar wind that was used for decades as the compositional signature, experiments such as CELIAS make possible the measurement of the coronal freeze-in charge states of minor solar wind ions such as Fe and O with high time resolution and the determination of the elemental composition that is characteristic for each type of solar wind. It is also pointed out in this section that compositional boundaries are found not only in CIRs but also, for example, between moderately steady slow solar wind and CME-related transient solar wind. Variations in solar wind composition are a steady tracer not only for the coronal hole boundaries but also for many other solar and coronal features and structures.

3.1. KINEMATIC CHARACTERISTICS OF SLOW AND FAST SOLAR WIND

CIRs are best identified as compressions on rising-speed portions of high-speed streams. Review articles on the measurements of the characteristic quantities of slow and fast solar wind have been published by Feldman *et al.* (1977), Marsch *et al.* (1982), and Schwenn (1990), based on data from the IMP 6, 7, and 8 and the Helios 1 and 2 missions. In Table I the bulk velocity v_p, the density n_p, the kinetic temperature T_p, the ratio of the kinetic temperatures parallel and perpendicular to the magnetic field, $T_{p\|}/T_{p\perp}$, the kinetic energy flux density $E_k = \frac{1}{2}\, n_p m_p v_p^3$ with m_p as proton mass, and the ratio of the kinetic and potential energy flux density, E_k/E_g with $E_g = n_p v_p G m_p M_s/R_\odot$ (M_s and $R_\odot$: mass and radius of the Sun, G: gravitational

TABLE I

Average values of basic solar wind parameters measured from Helios 1 and 2 between December 1974 and December 1976 and from IMP 6, 7, and 8 from 1972 to 1976 at 1 AU (from Feldman *et al.*, 1977, and Schwenn, 1990).

Parameter	slow (<400 km s^{-1})	fast (>600 km s^{-1})	all
v_p (km s^{-1})	327	702	468
n_p (cm^{-3})	8.3	2.73	6.1
T_p (10^3K)	34	230	120
$T_{p\|\|}/T_{p\perp}$	1.7	1.2	1.5
T_e (10^3K)	130	100	140
$T_{e\|\|}/T_{e\perp}$	1.2	1.6	1.18
E_k (10^{-7}J cm^{-2} s^{-1})	0.25	0.79	0.49
E_k/E_g	0.287	1.317	0.576
He^{2+}/H^+	0.038	0.048	0.047

constant) of the solar wind protons as well as the electron kinetic temperature T_e and the abundance ratio He^{2+}/H^+ are displayed.

In order to form a CIR the pattern of solar wind flow must be quai-stationary on a time scale comparable to one solar rotation or more. Previous studies have shown that this requirement is commonly met at low heliographic latitudes on the declining phase of the solar activity cycle and near solar minimum (*e.g.*, Snyder *et al.*, 1963; Gosling *et al.*, 1976). Figure 8 demonstrates via an autocorrelation analysis the persistence of the solar wind speed pattern on this time scale near the most recent solar minimum using data from the CELIAS experiment on SOHO.

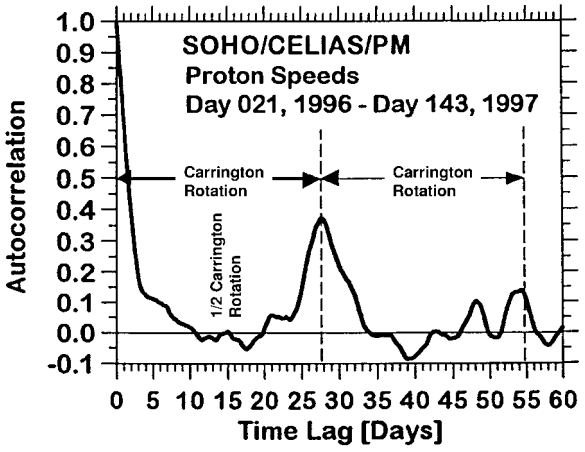

Figure 8. Autocorrelation function of proton speeds observed with CELIAS/PM (from Bochsler *et al.*, 1997).

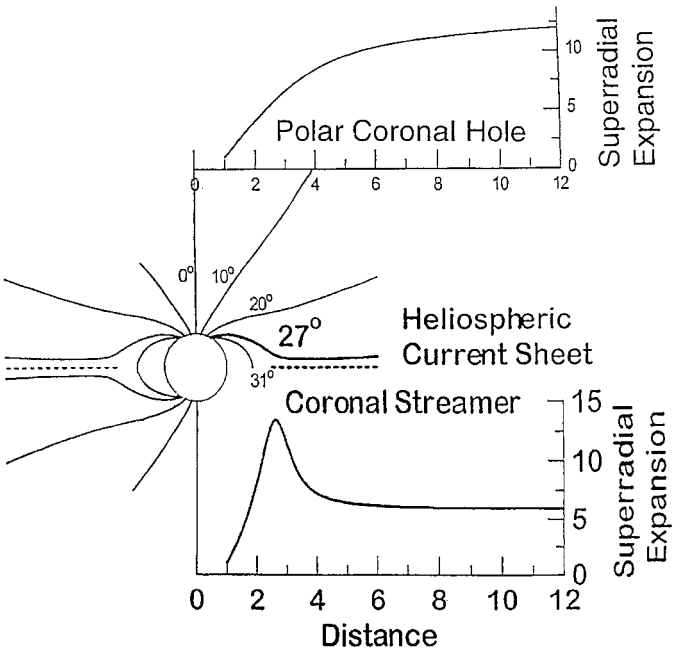

Figure 9. Magnetic field configuration of the corona during solar minimum (adapted from Wang and Sheeley, 1990, and Bodmer, 1996, see also Fig. 3). The slow solar wind originating near the solar equator and magnetic sector boundary has a much higher super-radial expansion above the closed magnetic coronal structures compared to the fast solar wind from polar coronal holes.

3.2. Compositional Characteristics of Slow and Fast Solar Wind

The minimum ratio He^{2+}/H^{+} mentioned in Table I commonly recurs at and near the HCS (Borrini *et al.*, 1981). Studies of von Steiger *et al.* (1995) revealed that the $^{4}He^{2+}$ depletion is caused by inefficient Coulomb coupling (Burgers, 1969; Geiss *et al.*, 1970) of the α-particles that have the least favorable drag factor, $Z^2/(2A - Z - 1)$ ($Q = Ze$: ion charge, $M = A$ amu: ion mass), among all minor solar wind ions. This effect can be explained by the geometry of the solar magnetic field (see Fig. 2 and 9). On the top of closed coronal magnetic field structures the slow solar wind has a strong super-radial expansion, as shown in Fig. 9, and hence a rapid decrease in the proton flux density. Therefore, the minor solar wind ions experience much less Coulomb drag compared to the situation in the fast solar wind. This even seems to influence the isotopic composition of slow and fast solar wind (Kallenbach *et al.*, 1998).

The different super-radial expansion profile of slow and fast solar wind also leads to different coronal altitudes and hence electron temperatures where the minor solar wind ion charge states freeze in, according to ionisation and recombination rates for electronic collisions from Arnaud and Rothenflug (1985). Slow solar

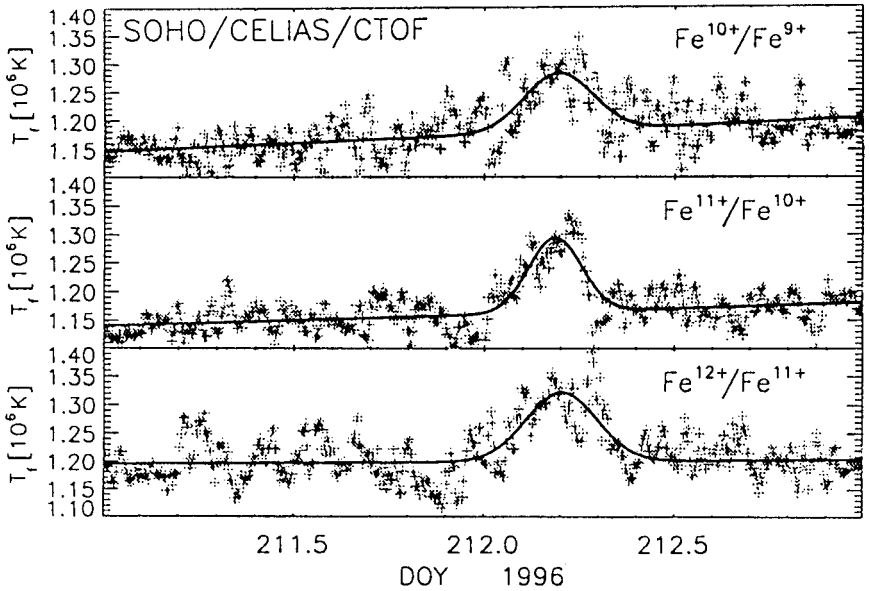

Figure 10. Charge state variations of Fe indicating a structure on the solar surface with a size of 15000 km corresponding to the size of a supergranular cell (from Aellig *et al.*, 1997).

wind in general shows higher freeze-in temperatures and wider distributions of charge states of Fe and O than fast solar wind. Recent SOHO observations with the Ultraviolet Coronal Spectrograph (UVCS) suggest that in coronal holes, the source region of the fast solar wind, minor solar wind ions are heated strongly at very close distances to the Sun down to $1.5\,R_\odot$ by ion cyclotron damping (Kohl *et al.*, 1997) but not in slow streams (Raymond *et al.*, 1997). This implies further differences between fast and slow solar wind at altitudes where the minor ion charge states freeze in (Wimmer-Schweingruber *et al.*, 1998).

These coronal freeze-in temperatures are on the order of 1 MK. The solar wind Fe charge states (Feldman *et al.*, 1981) measured with a time resolution of 5 minutes (Aellig *et al.*, 1998) by SOHO/CELIAS make it possible to resolve structures the size of the supergranular cells (Aellig *et al.*, 1997), as illustrated in Fig. 10. From these data an estimate for the strength of cross-field diffusion in the solar wind can be derived: The upper limit for the value of the perpendicular diffusion coefficient is $\kappa_\perp \leq 6 \times 10^{13} \mathrm{m^2 s^{-1}}$. This relatively small value explains why the plasmas of fast and slow solar wind stay fairly well separated in the CIRs, as reflected in the abrupt changes in entropy and compositional characteristics that occur at the stream interface.

Another difference in composition between fast and slow solar wind is the FIP (First Ionization Potential) effect (von Steiger and Geiss, 1989; Geiss *et al.*, 1995; von Steiger *et al.*, 1997). The change in FIP-related elemental composition in CIRs is discussed extensively in Wimmer-Schweingruber *et al.* (1997) as well as in

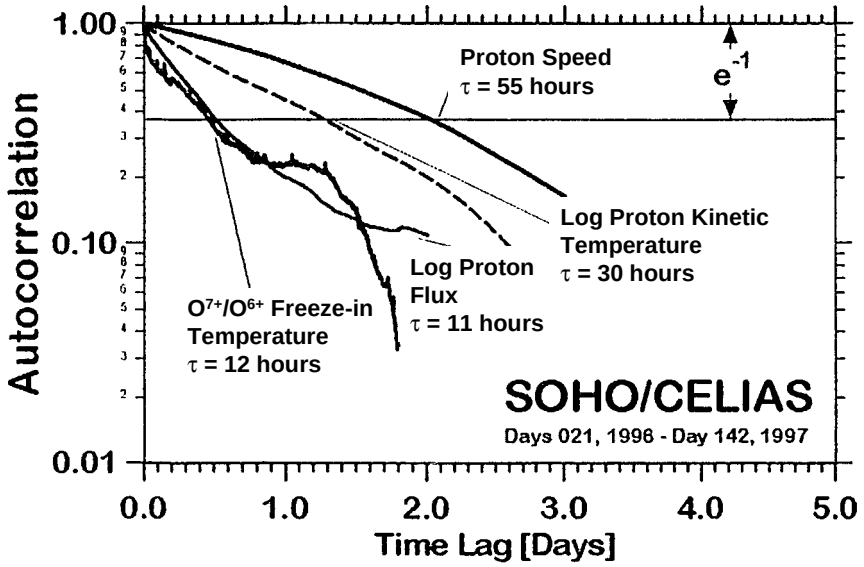

Figure 11. Persistence of proton dynamic properties and of oxygen freeze-in temperatures at 1 AU. The characteristic time scales are estimated from a linear fit to the logarithms of the autocorrelation functions (from Bochsler *et al.*, 1997).

this volume by Forsyth and Marsch (1999) and Crooker, Gosling *et al.* (1999). In general, the variations in FIP-related elemental composition and coronal freeze-in charge states are correlated because the solar wind flow is well guided by the magnetic field from the upper chromosphere and transition region, where the first ionisation takes place, up to the altitude where the charge states freeze in.

3.3. Persistence of Compositional and Kinematic Characteristics of the Solar Wind

In Sect. 3.1 the persistence of the solar wind proton speed with solar rotation was characterised. In this section we try to answer the question of how well variations in speed, temperature, and composition imprinted at the solar source and in the inner corona are conserved on their way to larger heliocentric distances. This has implications for the structure and sharpness of the compositional and kinematic signatures at SIs. This is a difficult question to answer because the influence of waves and turbulence on the compositional and kinematic signatures between fractions of an AU to the SOHO location at 1 AU are poorly known. A solar probe mission is needed to study these in-situ plasma properties close to the Sun. Such a mission could give information directly on the development of CIRs from their solar origin to the inner heliosphere.

At present there is one definite answer that can be given: The data in Fig. 11 show that on time scales that are short compared to the time of one Carrington rotation the autocorrelation functions of several compositional and kinematic pa-

rameters behave differently. The short-term autocorrelation time for the O^{7+}/O^{6+} ratio and the proton flux is considerably shorter than for the kinetic temperature and the proton speed. Bochsler *et al.* (1997) give two likely causes for the long persistence time of proton speeds:

1. Small-scale features are smoothed out, and
2. The stability of features with high specific energy content is enhanced.

The second statement also implies that the proton speeds are more important for the large-scale structure of the interplanetary medium.

For further interpretation two limiting cases can be considered: A) There is only little variation imprinted into composition, speed, and temperature at the solar source and in the inner corona (the autocorrelation time for constant parameters at the solar surface would be infinitely long), but waves and turbulence have more influence on the O^{7+}/O^{6+} ratio and on the proton flux than on proton speed and temperature. The short-term autocorrelation function then characterises the "noise" caused by waves and turbulence rather than the solar surface and inner coronal structure. B) There are strong variations imprinted into composition, speed, and temperature at the solar source and in the inner corona (the short-term autocorrelation time is short), but the smaller-scale signatures of speed and temperature smooth out faster in the solar wind flow than the signatures of the O^{7+}/O^{6+} ratio and the proton flux. This also implies that spatial structure sizes of the solar wind become larger on the way to the outer heliosphere. The largest structures are the regions of typical slow and fast solar wind that are separated by CIRs which can form shocks at several AU.

The result that structures with the size of a supergranular cell can be resolved with the Fe coronal freeze-in temperatures, corresponding to a time window of 2 hours at 1 AU, as reported in Sect. 3.2, suggests that the real situation is closer to scenario B). That implies that coronal freeze-in temperatures are good tracers for the structure of the plasma at the solar surface and in the inner corona, even in observations out at 1 AU. In any case, for both scenarios A) and B), the proton speed structures remain the most important feature for establishing the structure of the CIRs and the heliosphere. The scenario B) also matches the observations in an SI at 1 AU reported in the next section. Kinematic and compositional signatures become even sharper in SIs because of the plasma compression.

3.4. Stream Interfaces and Compositional Boundaries Between Different Types of Solar Wind

In the left panel a) of Fig. 12 a typical SI of a CIR is shown. The generally less-stationary structure of the slow solar wind is demonstrated in the right panel b), which also shows similarities and differences to SIs in CIRs and the overall wide applicability of minor solar wind ion signatures as diagnostic tool in interplanetary space: it displays the compositional boundaries (CB) between slow and fragmentary CME-related solar wind.

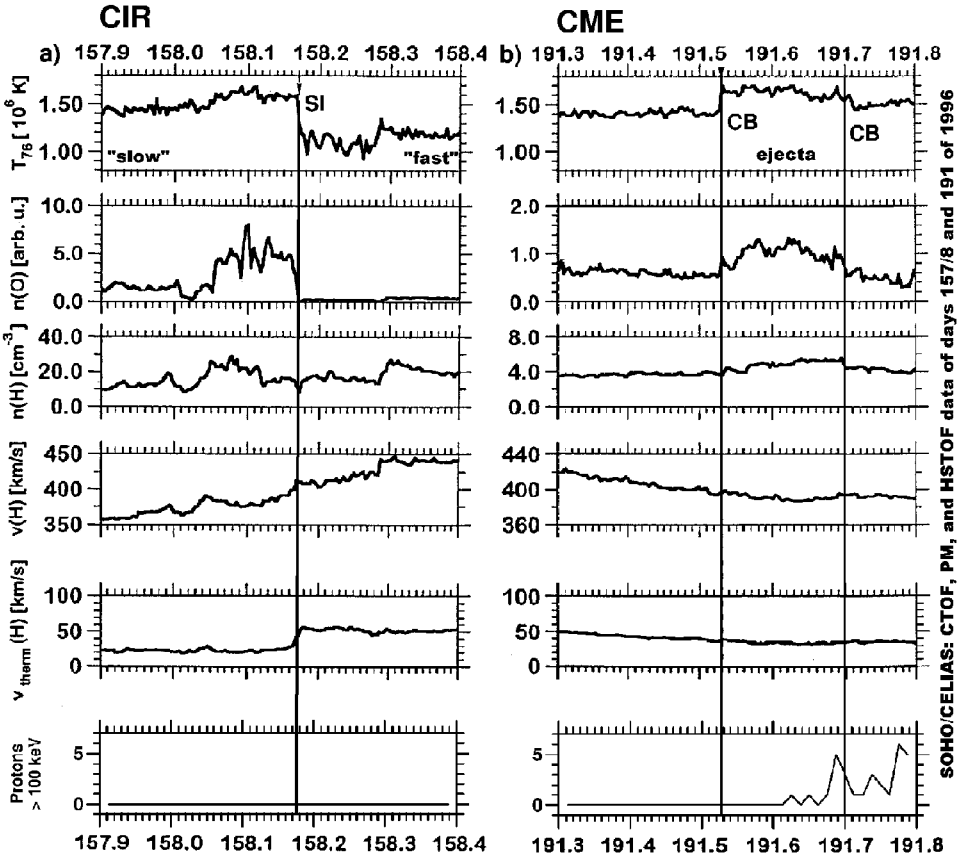

Figure 12. Left panel: Typical stream interface (SI) in a CIR at 1 AU (upper five data panels from Hefti, 1997). The interaction of the intermediate-speed stream with the low-speed solar wind causes a compression of the hydrogen and oxygen density. The kinetic temperature remains low in the compression region and increases in the intermediate stream within approximately 20 min. The sharpest separation between the two regimes is possible using T_f (O^{7+}/O^{6+}) (topmost panel). This parameter drops by 0.3 MK within a short time interval of 10 min. There is only a gradual transition within hours from low-speed solar wind with a proton bulk velocity of 350 km/s to intermediate-speed solar wind at 450 km/s. *Right panel:* Identification of compositional boundaries (CB) between slow solar wind and CME-related solar wind. The clearest signatures are given by the oxygen freeze-in charge states, density enhancements of protons and oxygen are also detected. The kinematic signatures alone would not provide clear evidence for the boundaries. However, at the trailing edge of the CME energetic particles are observed.

In a) the freeze-in temperature and oxygen density abruptly change within less than 10 minutes, whereas the proton density and bulk velocity only change within hours. This is at least partly due to the compression associated with the CIR that causes a deceleration of the fast wind and an acceleration of the slow wind. The step in the freeze-in temperature indicates how well the stream interface must have been conserved between the adjacent plasmas of different composition during the transit of more than four days from the freeze-in event at $\sim 2R_\odot$ to 1 AU. Still,

the compression characteristic for a CIR is reflected in the increase of the proton density by a factor of 2. The proton kinetic temperature also increases very quickly – within 20 minutes – by a factor of $\sim$2.

Panel b) of Fig. 12 shows a gradual transition from intermediate-speed to low-speed solar wind. There are two CBs belonging to the boundaries of the ejecta of a CME. The CBs in b) are not SIs and are not corotating because they are caused by a transient event. In b) there is only very slow change of the temperature, but considerable and abrupt change of the coronal freeze-in temperature.

It is evident that both kinematic and compositional signatures are precise diagnostic tools for the source regions of the solar wind which, depending on heliocentric distance and individual event, can have somewhat different characteristics. The appearance of these signatures in the SIs of CIRs is discussed in detail by Wimmer-Schweingruber *et al.* (1997) and Crooker, Gosling *et al.* (1999) in this volume. Using continuous Ulysses data from June 1992 to July 1993 Burton *et al.* (1999) demonstrated congruity between the traditional and compositional signatures. In so doing, they also demonstrated for the first time that the traditional density drop and temperature rise found in the compression region on the leading edge of a high-speed stream are nearly always matched by a density rise and temperature drop in the rarefaction region on the trailing edge.

4. CIRs in the Inner Heliosphere: A Summary of the Results From Helios

A. BALOGH and I. G. RICHARDSON

The dynamic evolution of adjacent solar wind streams emitted with different velocities from the corona is a continuous phenomenon all the way from the Sun. There are several key sets of observations (Pioneer 10 and 11, Voyager 1 and 2, Ulysses) which cover the evolution of interacting solar wind streams from the important baseline at 1 AU to well beyond 5 AU. For the inner solar system, for heliocentric distances less than 1 AU from the Sun, most observations come from the Helios 1 and 2 probes which had an eccentric orbit in the ecliptic plane, with perihelion close to 0.3 AU and aphelion at 1 AU. The Helios CIR observations represent the unique, if tenuous, bridge between near-solar conditions (see Sect. 2 and references therein) and the extensive observations during time periods near solar activity minimum at 1 AU and beyond documented in this volume and its references and discussed in the previous section with emphasis on the relationship between the different diagnostic tools for CIR studies at 1 AU and coronal and solar features. Our information about the properties and dynamics of the solar wind in the heliocentric range between 0.3 and 1 AU rely almost entirely on the two Helios spacecraft. In particular, given that well-developed, long-lasting CIRs are only observed during the declining and minimum phases of the solar cycle, the primary mission phases of Helios 1 and 2 have provided the first survey of the radial dependence of CIRs in this heliocentric range; the two spacecraft were launched in December 1974 and January 1976,

respectively, in the late declining phase of cycle 20 and at the following minimum phase, at the start of cycle 21. Note that stream-stream interactions do occur at all phases of the solar cycle, as velocity differentials at the coronal sources remain a feature of the solar wind at all times. However, when the coronal sources change significantly on the time scale of the solar rotation, as is the case around solar maximum, the interaction regions that result are transient and rarely form a corotating pattern lasting more than one solar rotation.

4.1. STREAM-STREAM INTERACTIONS AT < 1 AU

This summary of the Helios results relevant to the dynamics of CIRs is essentially based on the selected publications referenced in this section, in particular on Schwenn (1990) and the two volumes of the expanded results of Helios in the context of interplanetary physics (Schwenn and Marsch, 1990).

The Helios observations confirmed the stream structure of the solar wind to heliocentric distances down to 0.29 AU, as well as the association of high-speed streams with the equatorial extensions of coronal holes (Schwenn *et al.*, 1978; Burlaga *et al.*, 1978). A representative period of observations of the solar wind and the magnetic field observed by Helios 2 near solar minimum is shown in Fig. 13, covering a passage from aphelion at 1 AU to just past perihelion at 0.29 AU. In the bottom panel of Fig. 13, the ecliptic (azimuthal) angle of the magnetic field shows clearly the sector structure during this interval. The magnitude of the magnetic field increases, as expected, and shows a sequence of compressive features close to the sector boundaries and simultaneously with the density enhancements in the solar wind. In the upper three panels, the solar wind speed, density and proton temperature show a characteristic sequence of fast streams, separated by short passages through regions of slower and denser streams. A plot of the heliocentric distance of the observations is superimposed in the top panel of Fig. 13.

The solar/coronal context of the observations is illustrated in Fig. 14 by the coronal field map obtained from the photospheric magnetic field measurements, using the potential field, source surface model of Hoeksema *et al.* (1982). The period covered in Fig. 14 follows the period of the observations shown in Fig. 13; note that this is the first complete solar rotation for which such a coronal field map is available. But, given the stability of coronal structures near solar minimum in general, and the solar rotations following the one illustrated in Fig. 14, we can use it at least for qualitative comparison with the Helios solar wind and magnetic field observations shown in Fig. 13. There is a good match between the coronal magnetic field pattern and the solar wind observations in the preceding months. During this period of observations, Helios 2 "skimmed" the heliomagnetic equator, as represented by the coronal magnetic neutral line which is barely inclined, albeit with small amplitude folds due to a small contribution to coronal fields by quadrupole terms in the potential field expansion. During these observations, Helios 2 remained at a southern heliolatitude between 5° and 7°, except near peri-

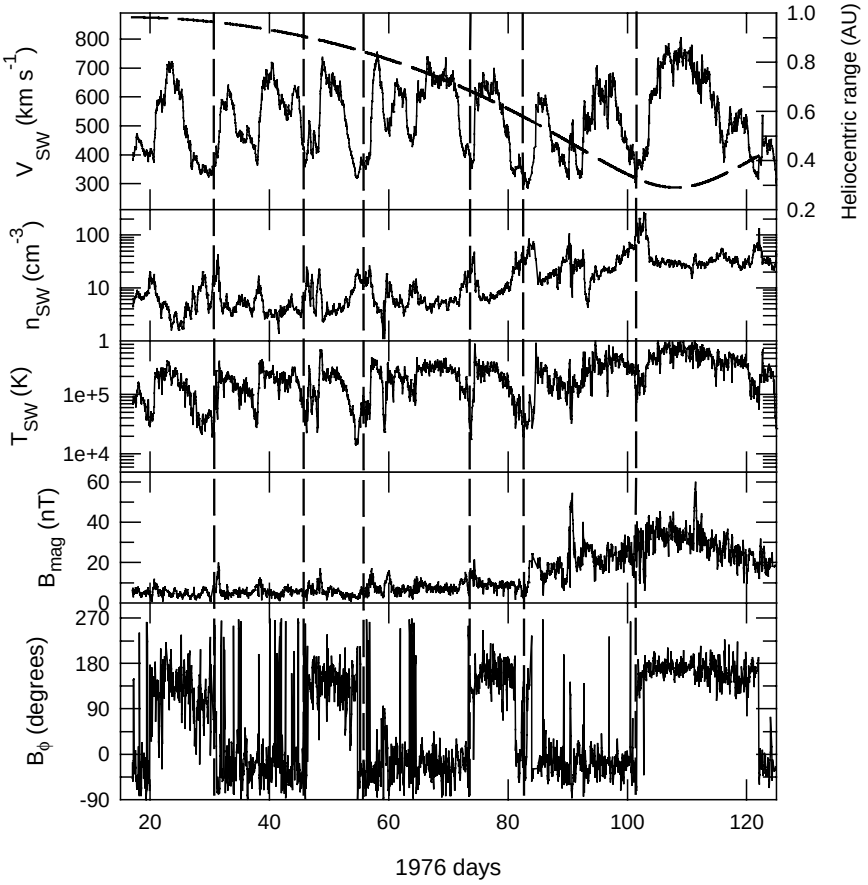

Figure 13. Helios 2 observations of the solar wind and the interplanetary magnetic field (IMF) during the first orbit from aphelion to perihelion in January to May 1976, showing the stream structure of the solar wind and the sector structure of the IMF. These observations, made in the ecliptic plane, are very characteristic of solar minimum when the sources of high-speed streams are close, in both hemispheres, to the solar equatorial plane. Note in particular the multiple encounters with slow streams in the negative magnetic sectors (indicated by the vertical dashed lines), due to the "skimming" of the Heliospheric Current Sheet by the orbit of Helios. (Solar wind data courtesy of R. Schwenn, Max-Planck-Insitut für Aeronomie, Lindau, magnetic field data courtesy of F. Neubauer, Universität zu Köln.)

helion (near the end of the period shown in Fig. 13) when its heliolatitude changed rapidly to a few degrees north of the solar equator. The relatively clear sector structure in Fig. 13 indicates the sharp boundary, at least on the large scale, between magnetic fields originating in the northern and southern hemispheres. However, the "skimming" effect is clearly seen in the solar wind parameters, as well as in the occasional, short duration magnetic polarity switches.

A notable feature of the observations is that in the negative sectors there are multiple peaks in the solar wind velocity, while the positive sectors contain only a

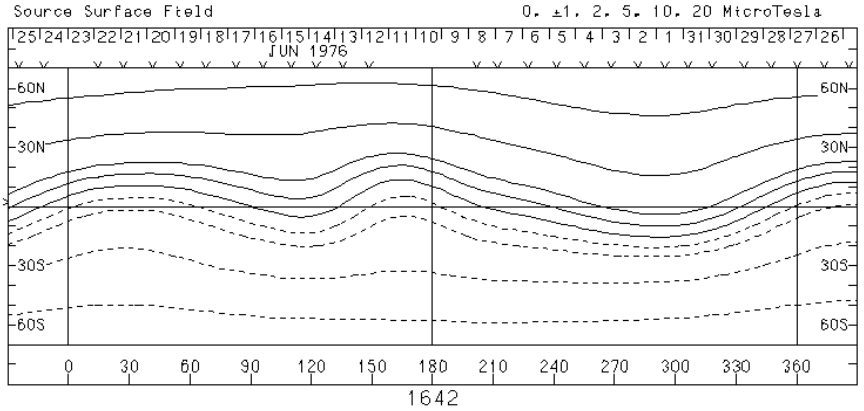

Figure 14. Potential field, source surface model of coronal magnetic fields calculated from photospheric measurements for May-June 1976, illustrating the reduced latitudinal extent of the likely location of the streamer belt (and of the source region of the slow solar wind) and the near-zero inclination of the magnetic neutral line to the solar equator. The folds represent the small contribution made by the higher order poles to the global coronal fields. This configuration, representative of solar minimum, is in agreement with the stream structure of the solar wind as measured by Helios 2, shown in Fig. 13, and with structure presented in Fig. 1. This is the first such coronal field map available for a complete solar rotation (courtesy of J. T. Hoeksema, Wilcox Solar Observatory, Stanford University).

single velocity peak ("mesa-like" at perihelion). This feature is well explained by reference to the coronal magnetic field map in Fig. 14. The heliomagnetic equator has a broad excursion to the south at around Carrington longitudes 270° to 330°; this leads to a positive magnetic sector and full immersion into the high-speed wind originating from the northern coronal hole. However, between Carrington longitudes 0° and 180°, there are two folds in the neutral sheet, both with small amplitude excursions to the north. While Helios 2 remains, on average, in the negative magnetic sector in this longitude range, it nevertheless repeatedly encounters at least the edges of slow streams (lying mostly southward of Helios 2), due to the proximity of the neutral line.

Similar observations have been presented by Burlaga *et al.* (1978) who examined in detail the stream structure in the early part of the Helios 1 mission, from launch in December 1974 to May 1995, beyond the first perihelion passage. Their observations showed a similar pattern of stream recurrence as shown in Fig. 13; in particular, one of the recurrent streams they examined showed a multi-peaked structure which they called a "compound" stream and associated it with an evolving pattern of coronal holes. While streams were found to recur from one solar rotation to the next, implying a stability in heliolongitude of the overall coronal pattern, the details of the solar wind (and magnetic field) observations in successive rotations were found to vary in response to changes in the boundary configuration of coronal holes.

In more general terms, at small heliospheric distances, less than 0.5 AU, the leading edges of many, but not all high-speed solar wind streams were found to be

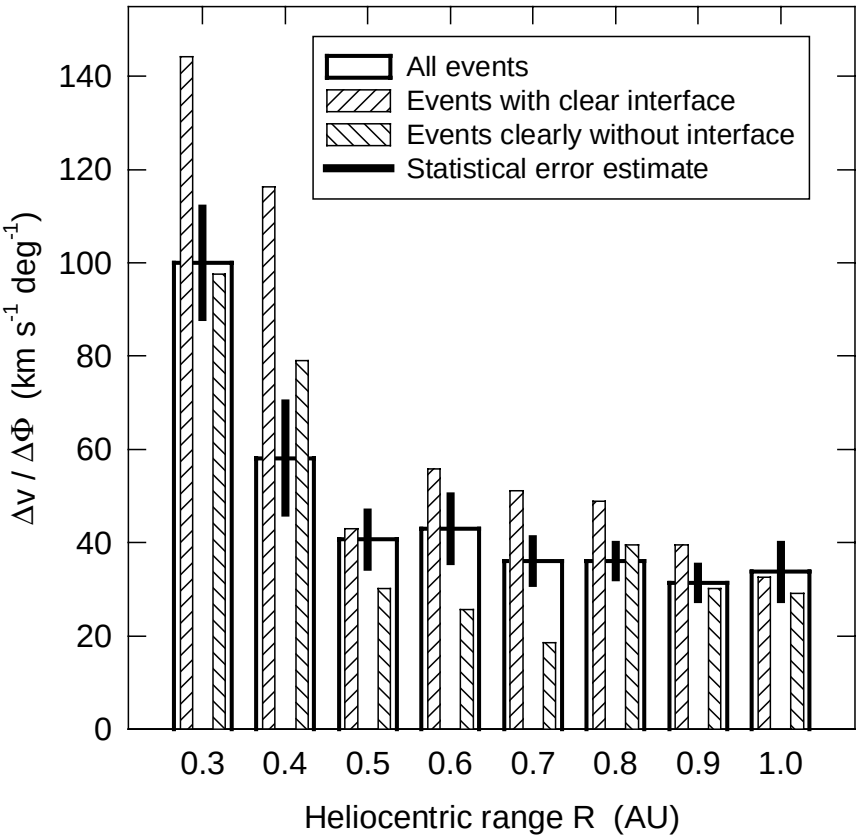

Figure 15. A statistical survey of the longitudinal speed gradients at the leading edges of fast solar wind streams, as a function of heliocentric distance, observed by Helios (adapted from Schwenn, 1990).

significantly steeper than at 1 AU. In addition, in many cases, high-speed streams had a "flat top" or "mesa-like" velocity profile, indicating a relatively constant, unevolved speed covering a range of tens of degrees in longitude, matching the width of the coronal hole source region. Compressive effects between streams were observed already at these distances, but were apparently limited by the still close to radially oriented Parker spiral direction. It was found, however, that beyond 0.5 AU, the compression between the streams became increasingly effective in shaping the profile of the solar wind parameters, due to the gradually increasing inclination of the Parker spiral with respect to the radial direction.

As noted in the above example of observations by Helios 2, solar minimum conditions have provided the opportunity to study the longitudinal dependence of the stream structure and the evolution of the resulting interaction regions very close to the heliomagnetic equator. A statistical evaluation of the solar wind speed gradients at the leading edges of fast streams, as a function of heliocentric distance, is shown in Fig. 15 (adapted from Schwenn, 1990). The gradients, evaluated with

respect to heliolongitude, are large at 0.3 AU (about 100 km $s^{-1}deg^{-1}$, on average), corresponding to a rise from the slow stream to the fast stream in only about 3° in heliolongitude. A specific high-speed stream observed by Helios 1 around perihelion and described by Burlaga *et al.* (1978) showed a very sharp leading edge, corresponding to a speed increase from 345 km/s to 625 km/s over 2.1° (a gradient in heliolongitude greater than 130 km $s^{-1}deg^{-1}$). Such relatively sharp longitudinal boundaries between the sources of slow and fast streams in the corona imply a clear distinction and a large velocity shear between fast and slow solar wind streams which are indeed observed. However, as discussed below, these gradients still allow considerable complexity (even a temporal dependence on short time scales) in the coronal structures which separate the solar wind source regions.

The orbit of Helios also allowed the study of the latitudinal boundaries of fast solar wind regions. As the region of origin of the slow wind surrounding the heliomagnetic equator (*i.e.* the coronal imprint of the HCS) contained near-equatorial folds (as illustrated in Fig. 14) the trajectory of the spacecraft crossed the latitudinal boundaries of coronal holes repeatedly. This study (see Schwenn, 1990) showed that these boundaries were quite sharp; the transition from slow- to high-speed solar wind occurred usually within a very few degrees in heliomagnetic latitude.

A more extensive study of the dependence of the solar wind speed on heliomagnetic latitude was carried out by Bruno *et al.* (1986), using data from the two Helios spacecraft and also from IMP 8 at 1 AU. The summary of their results is shown in Fig. 16 for 1976 and 1977. The speed gradient between the slow and fast solar wind streams is greater during the year of solar minimum (in 1976) than in the following year; the distinction between regions of slow and fast streams is quite obvious in both years. These statistical results in fact underestimate the latitudinal gradient; this is due partly the selection procedures adopted in the study and partly to the averaging used (this point was discussed in more detail by Schwenn, 1990). The speed gradients observed as a function of heliolatitude between actual streams are in fact generally significantly steeper than the statistically derived ones.

From about 0.5 AU, there is little change, on average, in the steepness of the velocity gradients. Nevertheless, on a number of occasions when the radial alignment of the two Helios spacecraft allowed the direct identification and comparison of high speed stream leading edges, there was evidence of renewed steepening with increasing heliocentric distance, due to increasing compression between the slow and the fast stream. This leads, at greater heliocentric distances, to the formation of shock pairs delimiting the CIRs. CIR-associated shocks are relatively rare at 1 AU (Gosling *et al.*, 1972); their occurrence was found to be even more infrequent along the Helios orbit. Despite the near-ideal conditions in which the very large number of CIRs were observed by Helios in the heliocentric range from 0.29 AU, only up to 11 forward shocks and even fewer reverse shocks could be attributed to stream-stream interaction (Schwenn, 1990). The shocks that were observed occured at distances greater than 0.6 AU, in fact most of them only close to perihelion at 1 AU (Richter *et al.*, 1985).

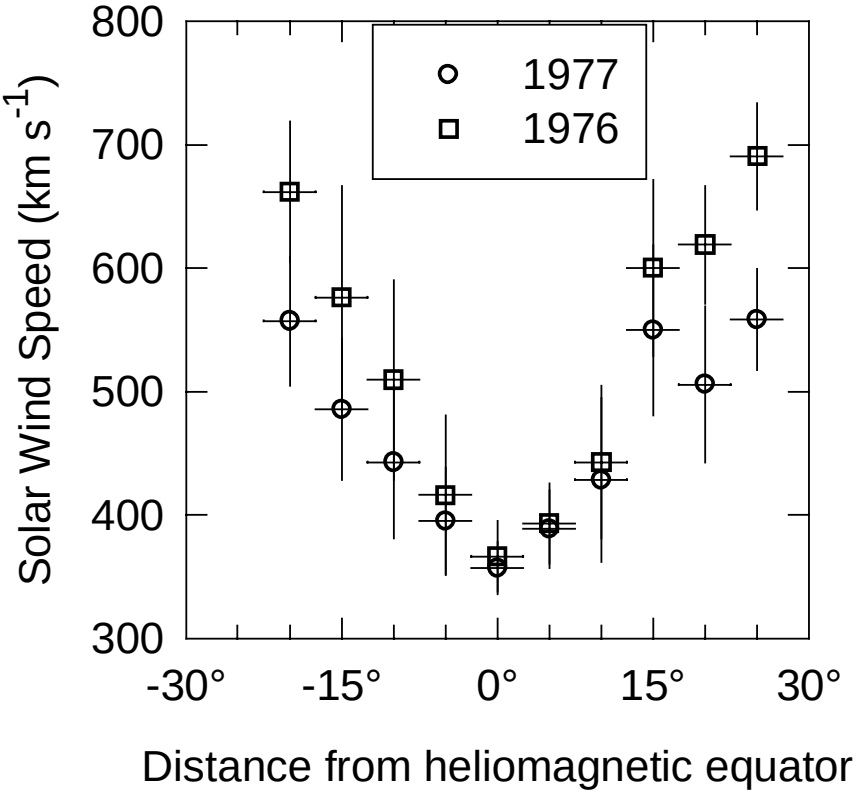

Figure 16. Solar wind velocities measured by Helios 1 and 2 and IMP 8 as a function of angular distance from the heliomagnetic equator, determined from the Maximum Brightness Contour measured by the HAO K-coronameter (based on Bruno *et al.*, 1986, but see discussion in Schwenn, 1990).

Figure 15 also shows explicitly the radial dependence of the steepness of those high-speed streams which either had a clear stream interface (defined as an abrupt increase in temperature and a decrease in solar wind density), or clearly had no such interface in the solar wind data. At 0.3 AU, this subset represented about a quarter of all observations of interacting streams, in contrast to 1 AU where half of the stream interfaces were clearly present or absent. By implication, neither the presence nor the absence of a slow-fast interface could be ascertained in 75% of the stream-stream interaction regions at 0.3 AU. We note that the presence of a detectable stream-stream interface was associated with significantly larger velocity gradients than the average in the observations at 0.3 and 0.4 AU. At distances greater than 0.5 AU, interaction regions with clearly identified interfaces had velocity gradients close to the average of all events.

The absence of a clear (abrupt) stream interface in the majority of CIRs observed by Helios, even close to the Sun, needs to be explained. This may have several reasons: SIs do not always need to have the same profile or steepness.

As mentioned above, only beyond 0.5 AU, the compression between the streams becomes increasingly effective in shaping the profile of the solar wind parameters. Also, the diagnostic tools of solar wind composition data (see Sect. 3) were not available at Helios. The generally expected tangential discontinuities (TD) at the SIs, separating solar wind plasma of different origins, are either difficult to identify or, more generally, are hidden effectively by the small scale structure within the CIRs. Flow deflections appear relatively small at small heliocentric distances and do not provide an unambiguous signature in general. It is likely, as pointed out by Schwenn (1990), that the transitions between regions of slow and fast wind streams in the corona can be quite complex (and not time stationary either), so that their signatures even close to the Sun can present a range of signatures on the small scale. This effect may be exaggerated by the "skimming" nature of the Helios orbit, so that the spacecraft may cut through the transition region at a highly oblique angle. The "high" longitudinal velocity gradients remain compatible with a relatively slow and complex transition implied on the small scale (of several degrees in longitude) between the coronal hole and the source region of the slow streams. The Helios observations clearly imply that, even close to the Sun, interfaces between slow and fast solar wind streams are usually complex; this result indicates that the identification of SIs further out from the Sun is not made difficult simply by interplanetary dynamic effects, but is likely to be the consequence of the nature of coronal structures themselves.

4.2. Particle Effects Associated with CIRs at ≤ 1 AU

Both low energy (few MeV) and high energy (cosmic ray) particle populations at ≤ 1 AU during solar minimum are predominantly ordered by CIRs and the related corotating high-speed streams. Sect. 11.6 of Kunow *et al.* (1991) provides a comprehensive summary of CIR-related particle observations at 0.3–1.0 AU from the Helios 1 and 2 spacecraft. Several aspects of these observations are illustrated in Fig. 17 which shows Helios 2 magnetic field, solar wind plasma, and energetic particle observations during a more than two-solar-rotation period in 1976 (part of the interval illustrated in Fig. 13) when the spacecraft moved from 1 AU to 0.65 AU. The magnetic field azimuth angle (ϕ) and solar wind speed (V_{SW}) data show that a recurrent two-sector structure and several corotating high-speed streams were present during this period. Low-energy particle enhancements (indicated by the 3.4–5.4 MeV proton intensity from the Goddard experiment) were associated with the corotating high-speed stream with outward ($\phi_{HSE} \sim 135^{\circ}$) magnetic field. In these and other similar particle enhancements, Kunow *et al.* (1977) and Van Hollebeke *et al.* (1978), observed positive radial MeV particle intensity gradients between the Helios spacecraft, IMP 7 and 8 at 1 AU, and Pioneer 11 at 3.8 AU. The gradients were steeper ($\sim$ 400%/AU) at < 1 AU than at 1–4 AU ($\sim$ 100%/AU). In addition, the particle spectra were shown to be independent of heliocentric distance between 0.3 and several AU. The observations suggested that

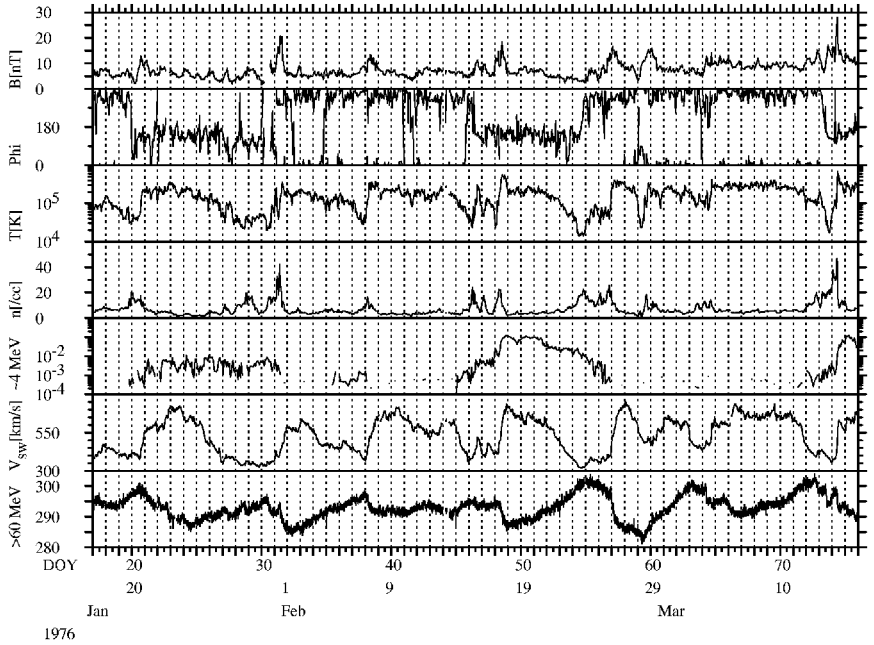

Figure 17. Helios 2 magnetic field, solar wind and energetic particle observations during a ~ 2 solar rotation period when the spacecraft moved from 1.0 to 0.65 AU.

these particles were accelerated at the CIR reverse shock at several AU and subsequently streamed sunward within the high speed stream. Kunow *et al.* (1977) also noted the presence of "precursor" ions, extending $\sim$1–2 days ahead of the leading edge of some streams (*e.g.*, on days 46–47 in Fig. 17), which had negative radial gradients between Helios 2 and IMPs 7 and 8, suggesting a different origin for these particles. The remaining high-speed streams in Fig. 17 were not associated with significant MeV particle enhancements. The reason for the absence of particle events in some streams, and their presence in others, requires further examination. Possible causes include differences in the stream structure and evolution, the interaction of streams in the outer heliosphere (which may influence the strength of the CIR shocks), and the disruption of long-lived streams by transient events (Kunow *et al.*, 1991).

The bottom panel shows recurrent galactic cosmic ray (GCR) density modulations, as measured by the counting rate (15-minute averages) of the anti-coincidence guard of the University of Kiel experiment, which responds to > 60 MeV particles. Previous studies using daily-averaged neutron monitor data at Earth have associated the onset of recurrent modulations with various structures, including stream leading edges, magnetic sector boundaries, magnetic field enhancements, and SIs (see references in Richardson *et al.*, 1996). Using high-time resolution guard data, Richardson *et al.* (1996) concluded that recurrent modulations at ≤ 1 AU typically commence at the leading edge of the high-speed stream, or at the enhancement

in field turbulence in the CIR (which often occurs at the stream leading edge). The cosmic ray density also tends to be anti-correlated with the solar wind speed, as is evident in Fig. 17, suggesting that increased cosmic ray convection plays a major role in the production of recurrent cosmic ray depressions, with the enhanced turbulence following the interface also contributing.

The amplitude of recurrent cosmic ray modulations in the inner heliosphere at solar minimum also exhibits a dependence on the 22-year global solar magnetic field polarity (A) cycle ($A > 0$ if the magnetic field points outward in the northern hemisphere), at least in the current and previous four solar minima (Richardson *et al.*, 1999). Observations from spacecraft and neutron monitors show that recurrent observations are $\sim$50% larger in $A > 0$ epochs. The reason for this epoch-dependence is unclear. The high-speed streams and CIRs do not appear to be necessarily stronger in $A > 0$ epochs – note, for example, the strong GCR modulations in the current solar minimum associated with modest streams (Heber *et al.*, 1997; Richardson *et al.*, 1999). The change in the GCR spectrum in alternate epochs is also not responsible since the amplitude dependence is observed in data covering a wide range of energies ($\sim$ 100 MeV–$\sim$ 13 GeV). An A-dependence might be expected if CIRs introduce enhanced particle scattering at low latitudes (*e.g.*, Kóta and Jokipii, 1991). However, stronger modulations would then be expected when cosmic rays enter the heliosphere along the equatorial regions (*i.e.*, in $A < 0$ epochs) than when they enter over the poles ($A > 0$) (*e.g.*, Fig. 3 of McKibben, Jokipii *et al.*, 1999, this volume). This is the opposite dependence to that which is actually observed. If effects due to local diffusion are predominant, then no A-dependence would be expected. In this case, another possibility is that particle transport parameters have a solar-field-dependence (*e.g.*, Chen and Bieber, 1993) such as to enhance the effect of cosmic ray convection in $A > 0$ epochs. A further complication is that the stream configuration also may play a role since large recurrent depressions can result from the combined effect of depressions in multiple, interacting streams.

5. Summary

A. BALOGH

Significant progress has been made in recent years in understanding the coronal origin of CIRs. This progress has been achieved by a firm characterisation of the fast solar wind and by the recognition that the slow solar wind is a complex mix of material emerging near the boundaries of coronal holes, as well as, in a manner yet to be clarified, in the form of transient "blobs" (Wang *et al.*, 1997) and CMEs. The task of the Working Group was (a) to take stock of the progress made in understanding the large scale structure of the corona in epochs characterised by the presence of large and stable coronal holes, (b) to examine in detail the nature

and characteristics of the SIs, and (c) to identify the questions which arise and can lead to a clarification of the origin of the slow solar wind.

– *The coronal origin of CIRs.* CIRs arise as a consequence of (a) solar wind streams of significantly different speeds emitted at the same solar latitude at adjacent longitudes, (b) the relative stability, over several solar rotations, of the coronal source regions, and (c) solar rotation, which brings solar wind streams of different speeds behind one another in the radial direction, and hence on a collision course. These three conditions are best fulfilled in the declining and minimum phases of the solar activity cycle, when fast streams, originating from relatively stable coronal holes, are emitted at low heliolatitudes where the slow solar wind streams also have their origin, above the near-equatorial streamer belt. The characteristics of the fast solar wind streams associated with large coronal holes have been well documented and are well understood, based on the long-term observations at 1 AU, and on observations in the inner heliosphere with the Helios spacecraft and in three dimensions by the Ulysses mission. The slow solar wind which emerges in the proximity of the streamer belt, with its highly variable characteristics, is much less understood. The natural variability apparent in CIR observations is the result of the spatial variability of coronal magnetic structures and their evolution on all time scales.
– *Modelling coronal magnetic and plasma structures.* Tracking the evolution of coronal structure in general, and of coronal holes in particular, has progressed significantly. Several complementary techniques are in use which are able, quite successfully, to extrapolate from photospheric observations of magnetic fields to predict open field regions in the upper corona, and to match these to space- and ground-based observations of coronal holes. These have been reviewed in Sect. 2 of this chapter. The increasing sophistication of coronal models is likely to lead to a better understanding of the source regions in the corona, in particular to the all-important boundary regions between open and closed magnetic field lines. It is not clear, however, to what extent the temporal dependences which are important both for the transition between open and closed field regions and the underlying dynamics of the streamers can be modelled in sufficient spatial and temporal detail at present.
– *Interplanetary dynamics in the inner heliosphere.* Helios observations in the inner heliosphere indicate a very good match of the stream structure to the coronal sources of high and low speed winds. There is evidence that the interaction between slow and fast solar wind streams depends on heliocentric distance as a function of the Parker spiral angle, in that the transitions between slow and high velocities are, on average, steeper at 0.3 AU than at 0.5 AU and beyond. There is also evidence for renewed steepening at greater distances, as compressive effects become more apparent. It would seem that SIs are at least as difficult to identify close to the Sun as at 1 AU. This reinforces the view expressed above that the critical question for SIs is the complexity (and

temporal, spatial variability) of the boundary between the coronal sources of high and low speed solar wind streams, rather than the dynamic effects due to the stream interaction process. While there was evidence in the Helios data for the occasional formation of corotating shocks at distances just inside 1 AU, such cases remain very rare, indicating that shock formation as a result of stream-stream interactions is a phenomenon belonging to distances greater than 1 AU (Gosling *et al.*, 1972).

– *Compositional signatures at SIs.* Measurements of the elemental and charge state composition of the solar wind have contributed significantly to the distinction between different types of solar wind streams. Compositional signatures are, at present, the best indicators of coronal origin in the solar wind plasma, and can be used in principle to detect and define the interfaces between different solar wind types. Given the complexity of the coronal boundaries between slow and fast wind, and the interplanetary dynamic effects which shape the SIs, the use of the diagnostic power of composition measurements has been used successfully in many cases to resolve the stream structure on scales which determine the SIs. The complexity of interfaces arises not only from the spatial complexity of the coronal structures between open and closed magnetic field lines, but also as a result of their temporal evolution and dynamics, resulting in apparently transient components in the slow solar wind which shape the initial conditions of the stream-stream interaction process. A further source of complexity is that coronal plasma emitted as slow solar wind clearly emerges from flux tubes of different composition and temperatures. Further studies of compositional signatures in the solar wind and their association with coronal processes which determine the characteristics of the emitted solar wind are needed and are likely to lead to a better understanding of interplanetary stream-stream interaction phenomena.

While CIRs are the results of interactions between slow and fast solar wind streams, their formation and evolution is a strong function of coronal morphology and the temporal characteristics of the source regions as well as of the transition region between closed and open magnetic field lines. The most important questions which are highlighted by a study of the solar origin of CIRs are related to the origin(s) of slow solar wind streams and to the details of coronal dynamics at the boundaries of coronal holes. Only a better understanding of the slow speed solar wind phenomenon can lead to new insights into the formation and initial dynamic development of CIRs.

Acknowledgements

Data from the National Solar Observatory at Kitt Peak are produced cooperatively by NSF/NOAO, NASA/GSFC, and NOAA/SEC. Data from the Mauna Loa Solar Observatory Mark III coronameter are courtesy of the High Altitude Observatory,

National Center for Atmospheric Research (NCAR), Boulder, Colorado, USA. NCAR is sponsored by NSF. The EIT data shown here are courtesy of the SOHO EIT Consortium. SOHO is a project of international cooperation between ESA and NASA. J. A. Linker and Z. Mikić were supported by the NASA and NSF. CELIAS is a joint effort of five hardware providing institutions under the direction of the Max Planck Institute for Extraterrestrial Physics, Garching, Germany, (prelaunch) and the University of Bern, Switzerland (postlaunch), and was supported by the Swiss National Science Foundation, by the PRODEX program of ESA, by NASA grant NAG5-2754, and by DARA, Germany, with grants 50 OC 89056 and 50 OC 9605.

References

Aellig, M. R., Grünwaldt, H., Bochsler, P., Wurz, P., Hefti, S., Kallenbach, R., Ipavich, F. M., Hovestadt, D., Hilchenbach, M., and the CELIAS team: 1997, 'Solar Wind Iron Charge States Observed with High Time Resolution with SOHO/CELIAS/CTOF', *ESA SP* **404**, 157–161.

Aellig, M. R., Grünwaldt, H., Bochsler, P., Wurz, P., Hefti, S., Kallenbach, R., Ipavich, F. M., and the CELIAS team: 1998, 'Iron Freeze-in Temperatures Measured by SOHO/CELIAS/CTOF', *J. Geophys. Res.* **103**, 17,215–17,222.

Altschuler, M. D., and Newkirk, G.: 1969, 'Magnetic Fields and the Structure of the Corona', *Sol. Phys.* **9**, 131–141.

Arnaud, M., and Rothenflug, R.: 1985, 'An Updated Evaluation of Recombination and Ionization Rates', *Astron. Astrophys. Suppl. Ser.* **60**, 425–457.

Billings, D. E.: 1966, *A Guide to the Solar Corona*, Academic Press.

Bodmer, R., and Bochsler, P.: 1998, 'Fractionation of Minor Ions in the Solar Wind Acceleration Process', *Phys. Chem. Earth* **23**, 683–688.

Bochsler, P., Hovestadt, D., Grünwaldt, H., Hilchenbach, M., Ipavich, F. M., Aellig, M. R., Axford, W. I., Balsiger, H., Bogdanov, A., Bürgi, A., Coplan, M. A., Galvin, A. B., Geiss, J., Gliem, F., Gloeckler, G., Hefti, S., Hsieh, K. C., Judge, D. L., Kallenbach, R., Klecker, B., Kucharek, H., Lasley, S. E., Lee, M. A., Litvinenko, Y., Livi, S., Managadze, G. G., Marsch, E., Möbius, E., Neugebauer, M., Ogawa, S., Paquette, J. A., Reiche, K.-U., Scholer, M., Verigin, M. I., Wilken, B., and Wurz, P.: 1997, 'The Sun at Minimum Activity: Results from the CELIAS Experiment on SOHO', *ESA SP* **404**, 37–43.

Borrini, G., Wilcox, J. M., Gosling, J. T., Bame, S. J., and Feldman, W. C.: 1981, 'Solar Wind Helium and Hydrogen Structure near the Heliospheric Current Sheet: A Signal of Coronal Streamers at 1 AU', *J. Geophys. Res.* **86**, 4,565–4,573.

Bruno, R., Villante, U., Bavassano, B., Schwenn, R., and Mariani, F.: 1986, 'In-situ Observations of the Latitudinal Gradients of the Solar Wind Parameters during 1976 and 1977', *Sol. Phys.* **104**, 431–445.

Burgers, J. M.: 1969, *Flow Equations for Composite Gases*, Academic Press, New York.

Burlaga, L. F., Ness, N. F., Mariani, F., Bavassano, B., Villante, U., Rosenbauer, H., Schwenn, R., and Harvey, J.: 1978, 'Magnetic Fields and Flows between 1 and 0.3 AU during the Primary Mission of Helios 1', *J. Geophys. Res.* **83**, 5,167–5,174.

Burton, M. E., Neugebauer, M., Crooker, N. U., Smith, E. J., and von Steiger, R.: 1999, 'Identification of Trailing Edge Solar Wind Stream Interfaces: A Comparison of Ulysses Plasma and Composition Measurements', *J. Geophys. Res.* **104**, 9,925–9,932.

Chen, J., and Bieber, J. W.: 1993, 'Cosmic Ray Anisotropies and Gradients in Three Dimensions', *Astrophys. J.* **405**, 375–389.

Crooker, N. U., Gosling, J. T., Bothmer, V., Forsyth, R. J., Gazis, P. R., Hewish, A., Horbury, T. S., Intriligator, D. S., Jokipii, J. R., Kóta, J., Lazarus, A. J., Lee, M. A., Lucek, E., Marsch, E., Posner, A., Richardson, I. G., Roelof, E. C., Schmidt, J. M., Siscoe, G. L., Tsurutani, B. T., and Wimmer-Schweingruber, R. F.: 1999, 'CIR Morphology, Turbulence, Discontinuities, and Energetic Particles', *Space Sci. Rev.*, this volume, 179–220.

Feldman, W. C., Asbridge, J. R., Bame, S. J., and Gosling, J. T.: 1977, 'Plasma and Magnetic Fields from the Sun', *in* O. R. White (ed.), *The Solar Output and its Variations*, Colorada Associated University Press, Boulder, pp. 351–381.

Feldman, W. C., Asbridge, J. R., Bame, S. J., Fenimore, E. E., and Gosling, J. T.: 1981, 'The Solar Origins of Solar Wind Interstream Flows: Near-Equatorial Coronal Streamers', *J. Geophys. Res.* **86**, 5,408–5,416.

Fisk, L. A., and Jokipii, J. R.: 1999, 'Mechanisms for Latitudinal Transport of Energetic Particles in the Heliosphere', *Space Sci. Rev.*, this volume, 115–124.

Fisk, L. A., Schwadron, N. A., and Zurbuchen, T. H.: 1998, 'On the Slow Solar Wind', *Space Sci. Rev.* **86**, 51–60.

Forsyth, B., and Marsch, E.: 1999, 'Solar Origin and Interplanetary Evolution of Stream Interfaces', *Space Sci. Rev.*, this volume, 7–20.

Geiss, J., Hirt, P., and Leutwyler, H.: 1970, 'On Acceleration and Motion of Ions in Corona and Solar Wind', *Sol. Phys.* **12**, 458–484.

Geiss, J., Gloeckler, G., von Steiger, R., Balsiger, H., Fisk, L. A., Galvin, A. B., Ipavich, F. M., Livi, S., McKenzie, J. F., Ogilvie, K. W., and Wilken, B.: 1995, 'The Southern High-Speed Stream: Results from the SWICS Instrument on Ulysses', *Science* **268**, 1,033–1,036.

Gloeckler, G., Fisk, L. A., Hefti, S., Schwadron, N. A., Zurbuchen, T. H., Ipavich, F. M., Geiss, J., Bochsler, P., and Wimmer-Schweingruber, R. F.: 1999, 'Unusual Composition of the Solar Wind in the May 2–3, 1998, CME Observed with SWICS on ACE', *Geophys. Res. Lett.* **157**, 157–160.

Gosling, J. T.: 1997, 'Physical Nature of the Low-speed Solar Wind', *in* S. R. Habbal (ed.), *AIP Conference Proceedings* **385**, AIP, Woodbury, New York, pp. 17–24.

Gosling, J. T., Hundhausen, A. J., Pizzo, V., and Asbridge, J. R.: 1972, 'Compressions and Rarefactions in the Solar Wind: Vela 3', *J. Geophys. Res.* **77**, 5,442–5,454.

Gosling, J. T., Asbridge, J. R., Bame, S. J., and Feldman, W. C.: 1976, 'Solar Wind Speed Variations: 1962–1974', *J. Geophys. Res.* **81**, 5,061–5,070.

Gosling, J. T., Asbridge, J. R., Bame, S. J., and Feldman, W. C.: 1978, 'Solar Wind Stream Interfaces', *J. Geophys. Res.* **83**, 1,401–1,412.

Gosling, J. T. and Pizzo, V.: 1999, 'Formation and Evolution of Corotating Interaction Regions and Their Three-Dimensional Structure', *Space Sci. Rev.*, this volume, 21–52.

Heber, B., Bothmer, V., Dröge, W., Kunow, H., Müller-Mellin, R., Posner, A., Ferrando, P., Raviart, A., Paizis, C., McComas, D., Forsyth, R. J., Szabo, A., and Lazarus, A. J.: 1997, 'Spatial Evolution of 26-day Recurrent Galactic Cosmic Ray Decreases: Correlated Ulysses COSPIN/KET and SOHO COSTEP Observations', *ESA SP* **415**, 331–340.

Hefti, S.: 1997, 'Solar Wind Freeze-in Temperatures and Fluxes Measured with SOHO/CELIAS/CTOF and Calibration of the CELIAS Sensors', *PhD Thesis*, University of Bern, Switzerland.

Hoeksema, J. T., Wilcox, J. M., and Scherrer, P. H.: 1982, 'Structure of the Heliospheric Current Sheet in the Early Portion of Sunspot Cycle 21', *J. Geophys. Res.* **87**, 10,331-10,338.

Hoeksema, J. T., Wilcox, J. M., and Scherrer, P. H.: 1983, 'The Structure of the Heliospheric Current Sheet: 1978–1982', *J. Geophys. Res.* **88**, 9,910–9,918.

Hovestadt, D., Hilchenbach, M., Bürgi, A., Klecker, B., Laeverenz, P., Scholer, M., Grünwaldt, H., Axford, W. I., Livi, S., Marsch, E., Wilken, B., Winterhoff, H. P., Ipavich, F. M., Bedini, P., Coplan, M. A., Galvin, A. B., Gloeckler, G., Bochsler, P., Balsiger, H., Fischer, J., Geiss, J.,

Kallenbach, R., Wurz, P., Reiche, K.-U., Gliem, F., Judge, D. L., Ogawa, H. S., Hsieh, K. C., Möbius, E., Lee, M. A., Managadze, G. G., Verigin, M. I., and Neugebauer, M.: 1995, 'Charge, Element, and Isotope Analysis System onboard SOHO', *Sol. Phys.* **162**, 441–481.

Kallenbach, R., Ipavich, F. M., Kucharek, H., Bochsler, P., Galvin, A.B., Geiss, J., Gliem, F., Gloeckler, G., Grünwaldt, H., Hefti, S., Hilchenbach, M., and Hovestadt, D.: 1998, 'Fractionation of Si, Ne, and Mg Isotopes in the Solar Wind as Measured by SOHO/CELIAS/MTOF', *Space Sci. Rev.* **85**, 357–370.

Kohl, J. L., Noci, G., Antonucci, E., Tondello, G., Huber, M.C.E., Gardner, L. D., Nicolosi, P., Strachan, L., Fineschi, S., Raymond, J. C., Romoli, M., Spadaro, D., Panasyuk, A., Siegmund, O.H.W., Benna, C., Ciaravella, A., Cranmer, S. R., Giordano, S., Karovska, M., Martin, R., Michels, J., Modigliani, A., Naletto, G., Pernechele, C., Poletto, G., and Smith, P. L.: 1997, 'First Results from the SOHO Ultraviolet Coronagraph Spectrometer', *Sol. Phys.* **175**, 613–644.

Kóta, J., and Jokipii, J. R.: 1979, 'The Role of Corotating Interaction Regions in Cosmic Ray Modulation', *Geophys. Res. Lett.* **18**, 1797–1800.

Kunow, H., Wibberenz, G., Green, G., Müller-Mellin, R., Witte, M., Hempe, H., Mewaldt, R. A., Stone, E. C., and Vogt, R. E.: 1977, 'Simultaneous Observations of Cosmic Ray Particles in a Corotating Interplanetary Structure at Different Solar Distances between 0.3 and 1 AU and IMP 7 and 8', *Proc. Int. Cosmic Ray Conf. (Plovdiv)* **3**, 227–230.

Kunow, H., Wibberenz, G., Green, G., Müller-Mellin, R., and Kallenrode, M.-B.: 1991, 'Energetic Particles in the Inner Solar System', *in* R. Schwenn and E. Marsch (eds.), *Physics of the Inner Heliosphere II*, Physics and Chemistry in Space–Space and Solar Physics **21**, Springer-Verlag, pp. 243–342.

Linker, J. A., Mikić, Z., and Schnack, D. D.: 1996, 'Coronal Modeling and Space Weather Prediction', *in* K. S. Balasubramaniam, S. L. Keil, and R. N. Smartt (eds), *Solar Drivers of Interplanetary and Terrestrial Disturbances*, *Astron. Soc. Pac. Conf.* **95**, 208.

Linker, J. A., and Mikić, Z.: 1997, 'Extending Coronal Models to Earth Orbit', *in* N. U. Crooker, J. A. Joselyn, and J. Feynman (eds), *Coronal Mass Ejections*, Geophys. Monogr. Ser. **99**, p. 269.

Linker, J. A., Mikić, Z. Biesecker, D. A., Forsyth, R. J., Gibson, S. E., Lazarus, A. J., Lecinski, A., Riley, P., Szabo, A., and Thompson, B. J.: 1999, 'Magnetohydrodynamic Modeling of the Solar Corona during Whole Sun Month', *J. Geophys. Res.* **104**, 9,809–9,830.

Marsch, E., Mühlhäuser, K. H., Schwenn, R., Rosenbauer, H., Pilipp, W., and Neubauer, F. M.: 1982, 'Solar Wind Protons: Three-Dimensional Velocity Distributions and Derived Plasma Parameters Measured between 0.3 and 1 AU', *J. Geophys. Res.* **87**, 52–72.

McKibben, R. B., Jokipii, J. R., Burger, R. A., Heber, B., Kóta, J., McDonald, F. B., Paizis, C., Potgieter, M. S., and Richardson, I. G.: 1999, 'Modulation of Cosmic Rays and Anomalous Components by CIRs', *Space Sci. Rev.*, this volume, 307–326.

Mikić, Z., and Linker, J. A.: 1996, 'The Large-Scale Structure of the Solar Corona and Inner Heliosphere', *in* D. Winterhalter, J. T. Gosling, S. R. Habbal, W. S. Kurth, and M. Neugebauer (eds), *Solar Wind Eight*, AIP Proceedings, Woodbury, New York, p. 104.

Mikić, Z., Linker, J. A. Schnack, D. D., Lionello, R., and Tarditi, A.: 1999, 'Magnetohydrodynamic Modeling of the Global Solar Corona', *Phys. Plasmas* in press.

Parker, E.N.: 1958, 'Dynamics of the Interplanetary Gas and Magnetic Fields', *Astrophys. J.* **128**, 664.

Phillips, J. L., Bame, S. J., Barnes, A., Barraclough, B. L., Feldman, W. C., Goldstein, B. E., Gosling, J. T., Hoogeveen, G. W., McComas, D. J., Neugebauer, M., and Suess, S. T.: 1995, 'Ulysses Solar Wind Plasma Observations from Pole to Pole', *Geophys. Res. Lett.* **22**, 3301–3304.

Posner, A., Bothmer, V., Thompson, B. J., Kunow, H., Heber, B., Müller-Mellin, R., Lazarus, A. J., Szabo, A., Mikić, Z., and Linker, J. A.: 1999, 'In-ecliptic CIR-associated Energetic Particle Events and Polar Coronal Hole Structures: SOHO/COSTEP Observations for the Whole Sun Month Campaign', *J. Geophys. Res.* **104**, 9,881–9,890.

Raymond, J. C., Kohl, J. L., Noci, G., Antonucci, E., Tondello, G., Huber, M.C.E., Gardner, L. D., Nicolosi, P., Fineschi, S., Romoli, M., Spadaro, D., Siegmund, O.H.W., Benna, C., Ciaravella, A., Cranmer, S. R., Giordano, S., Karovska, M., Martin, R., Michels, J., Modigliani, A., Naletto, G., Panasyuk, A., Pernechele, C., Poletto, G., Smith, P. L., Suleiman, R. M., and Strachan, L.: 1997, 'Composition of Coronal Streamers from the SOHO Ultraviolet Coronagraph Spectrometer', *Sol. Phys.* **175**, 645–665.

Richardson, I. G., Wibberenz, G., and Cane, H. V.: 1996, 'The Relationship between Recurring Cosmic Ray Depressions and Corotating Solar Wind Streams at ≤ 1 AU: IMP 8 and Helios 1 and 2 Anticoincidence Guard Rate Observations', *J. Geophys. Res.* **101**, 13,483–13,496.

Richardson, I. G., Cane, H. V., and Wibberenz, G.: 1999, 'Corotating Cosmic Ray Depressions near the Ecliptic during Five Solar Minima: Evidence for a 22-Year Dependence', *J. Geophys. Res.* **104**, 12,549–12,561.

Richter, A. K., Hsieh, K. C., Luttrell, A. H., Marsch, E., Schwenn, R.: 1985, 'Review of Interplanetary Shock Phenomena near and within 1 AU', *in* B. T. Tsurutani and R. G. Stone (eds.), *Collisionless Shocks in the Heliosphere: Reviews of Current Research*, Geophysical Monograph, American Geophysical Union, pp. 33–50.

Schatten, K. H., Wilcox, J. M., and Ness, N.: 1969, 'A Model of Interplanetary and Coronal Magnetic Fields', *Sol. Phys.* **6**, 442–455.

Schatten, K. H.: 1971, 'Current Sheet Magnetic Model of the Solar Corona', *Cosmic Electrodyn.* **4**, 11.

Schwenn, R., Montgomery, M. D., Rosenbauer, H., Miggenrieder, H., Mülhauser, K. H., Bame, S. J., Feldman, W. C., and Hansen, R. T.: 1978, 'Direct Observation of the Latitudinal Extent of a High Speed Stream in the Solar Wind', *J. Geophys. Res.* **83**, 1,011–1,017.

Schwenn, R.: 1990, 'Large-Scale Structure of the Interplanetary Medium', *in* Schwenn and Marsch (1990), pp. 99–181.

Schwenn, R., and Marsch, E. (eds.): 1990, *Physics of the Inner Heliosphere I*, Physics and Chemistry in Space - Space and Solar Physics **20**, Springer-Verlag.

Snyder, C. W., Neugebauer, M., and Rao, U. R.: 1963, 'The Solar Wind Velocity and its Correlation with Cosmic-Ray Variations and with Solar and Geomagnetic Activity', *J. Geophys. Res.* **68**, 6,361–6,370.

Usmanov, A. V.: 1996, 'A Global 3-D MHD Solar Wind Model with Alfvén Waves', *in* D. Winterhalter, J. T. Gosling, S. R. Habbal, W. S. Kurth, and M. Neugebauer (eds.), *Solar Wind Eight*, AIP Proceedings, Woodbury, New York, p. 141.

Van Hollebeke, M.A.I., McDonald, F. B., and von Rosenvinge, T. T.: 1978, 'The Radial Variation of Corotating Particle Streams in the Inner and Outer Solar System', *J. Geophys. Res.* **83**, 4,723–4,731.

von Steiger, R., and Geiss, J.: 1989, 'Supply of Fractionated Gases to the Corona', *Astron. Astrophys.* **225**, 222–238.

von Steiger, R., Wimmer-Schweingruber, R. F., Geiss, J., and Gloeckler, G.: 1995, 'Abundance Variations in the Solar Wind', *Adv. Space Res.* **15**, (7)3–(7)12.

von Steiger, R., Geiss, J., and Gloeckler, G.: 1997, 'Composition of the Solar Wind', *in* J. R. Jokipii, C. P. Sonett, and M. S. Giampapa (eds.), *Cosmic Winds and the Heliosphere*, Arizona Press, Tucson, AZ, USA, pp. 581–616.

von Steiger, R.: 1998, 'Composition Aspects of the Upper Solar Atmosphere', *Space Sci. Rev.* **85**, 407–418.

Wang, Y.-M., and Sheeley, N. R., Jr.: 1988, 'The Solar Origin of Long-Term Variations of the Interplanetary Magnetic Field Strength', *J. Geophys. Res.* **93**, 11,227–11,236.

Wang, Y.-M., and Sheeley, N. R., Jr.: 1990, 'Solar Wind Speed and Coronal Flux-Tube Expansion', *Astrophys. J.* **355**, 726–732.

Wang, Y.-M., and Sheeley, N. R., Jr.: 1992, 'On Potential Field Models of the Solar Corona', *Astrophys. J.* **392**, 310–319.

Wang, Y.-M., and Sheeley, N. R., Jr.: 1994, 'Global Evolution of Interplanetary Sector Structure, Coronal Holes, and Solar Wind Streams during 1976-1993: Stackplot Displays Based on Solar Magnetic Observations', *J. Geophys. Res.* **99**, 6,597–6,608.

Wang, Y.-M., and Sheeley, N. R., Jr.: 1995, 'Solar Implications of Ulysses Interplanetary Field Measurements', *Astrophys. J.* **447**, L143–L148.

Wang, Y.-M., Sheeley, N. R., Jr., Howard, R. A., Kraemer, J. R., Rich, N. B., Andrews, M. D., Brueckner, G. E., Dere, K. P., Koomen, M. J., Korendyke, C. M., Michels, D. J., Moses, J. D., Paswaters, S. E., Socker, D. G., Wang, D., Lamy, P. L., Llebria, A., Vibert, D., Schwenn, R., and Simnett, G. M.: 1997, 'Origin and Evolution of Coronal Streamer Structure during the 1996 Minimum Activity Phase', *Astrophys. J.* **485**, 875–889.

Wang, Y.-M., Sheeley, N. R., Jr., Walters, J. H., Brueckner, G. E., Howard, R. A., Michels, D. J., Lamy, P. L., Schwenn, R., and Simnett, G. M.: 1995, 'Origin of Streamer Material in the Outer Corona', *Astrophys. J.* **498**, L165–L168.

Wimmer-Schweingruber, R. F., von Steiger, R., and Paerli, R.: 1997, 'Solar Wind Stream Interfaces in Corotating Interaction Regions: SWICS/Ulysses Results', *J. of Geophys. Res.* **102**, 17,407–17,417.

Wimmer-Schweingruber, R. F., von Steiger, R., Geiss, J., Gloeckler, G., Ipavich, F. M., and Wilken, B.: 1998, 'O^{5+} in High Speed Solar Wind Streams: SWICS/ULYSSES Results', *Space Sci. Rev.* **85**, 387–396.

Zhao, X. P., Hoeksema, J. T., and Scherrer, P. H.: 1999, 'Changes of the Boot-Shaped Coronal Hole Boundary during Whole Sun Month near Sunspot Minimum', *J. Geophys. Res.* **104**, 9,735–9,751.

Address for Offprints: A. Balogh, Blackett Laboratory, Imperial College, London SW7 2BZ, United Kingdom; a.balogh@ic.ac.uk